Rebecca Dell
Scott Polar Research Institute
University of Cambridge
Lensfield Road
Cambridge CB2 1ER
United Kingdom

Tel: +44 (0) 7925618105
Email: rld46@cam.ac.uk

30th March 2020

Dear Dr Whitehouse,

RE: Response to Reviewer Comments

We have received two reviews of our manuscript entitled 'Lateral meltwater transfer across an Antarctic ice shelf (tc-2019-316). Overall, both reviews were supportive of the paper and its relevance to the wider research community.

Both reviewer's comments have been extremely helpful in further improving the manuscript. The specific changes made can be found in our responses below. Referee comments are italicised in *blue*, our responses are in black. Please also find attached a revised manuscript with all tracked changes. When referring to page numbers in the below text, these will be in line with the page numbers on the 'tracked changes' manuscript.

Thank you for taking your time to consider our revised manuscript, we hope it is now acceptable for publication.

Sincerely,

Rebecca Dell and co-authors

Response to Reviewer Comments – Reviewer 1

Overall Comments

This manuscript presents a quantitative analysis of meltwater distribution, storage and transfer on the Nivlisen Ice Shelf, Dronning Maud Land in East Antarctica during one melt season (2016-2017). The authors use a modified version of a previously published algorithm to classify meltwater into four different categories from Landsat-8 and Sentinel-2 imagery and track meltwater area and volume through the melt season. Meltwater has been linked to the instability and collapse of Antarctic ice shelves, but detailed observations of the seasonal evolution of meltwater on ice shelves in Antarctica are lacking. Therefore, it is my view that the findings from this manuscript are of broad interest to the cryosphere community. In general, the manuscript is well-written and clearly structured and the rationale for the study is well justified. The quantification of meltwater area and volume stored and transferred on the ice shelf during one melt season builds upon previous work that has identified surface meltwater systems present on numerous Antarctic outlet glaciers and ice shelves (Langley et al., 2016; Kingslake et al., 2017; Stokes et al., 2019).

We thank Reviewer 1 for this positive overview and their further constructive review.

Major Comments

It is not immediately clear how the authors have adapted the previously published FASTER algorithm into the algorithm used here, FASTISh, and its novelty could be communicated more clearly.

And also minor comments: *Line 90: See general comment above about highlighting the difference in algorithms.*

Line 278: I think this needs to be better highlighted that this is what sets FASTISh apart from the previous algorithm, FASTER (which did not track water body type).

We agree with these comments, and have made the differences between the FASTER and FASTISh algorithms clearer (lines 123-133), we have also added a paragraph justifying the need for these adaptations (lines 100-117).

Its ability to differentiate between lakes and streams represents an important advance because it gives insight into the lateral transport of meltwater across ice shelves, not just the in-situ storage, but this needs to be made clearer in the Introduction.

We have now made this difference between FASTER and FASTISh clearer in introduction (lines 123-133) and also in the abstract (lines 26-27).

On a related note, I am slightly apprehensive about the binary classification of lake versus stream – what about elongate, linear lakes, which are common on Antarctic ice shelves?

Based on our current level of analysis, we now agree that it is not possible to confidently categorise water bodies as lakes or streams. We have therefore re-named our categories to purely reflect the geometry of the water bodies, which are now classified as either circular or linear, regardless of whether they contain ponded or flowing water. These adjustments have been made where appropriate throughout the manuscript.

There is a lack of discussion of the limitations associated with the methods used in Section 3, including classifying water body types, and applying the depth retrieval algorithm. The depth algorithm is known to only retrieve depths up to a certain point because rapid attenuation of red wavelengths means that only shallower lakes can be measured in this band (Pope et al., 2016), and makes several assumptions (see Sneed and Hamilton, 2011). The reader should be made aware of these limitations.

As above, we have changed the water body type definitions from 'lakes' and 'streams' to 'circular' and 'linear' features; this should remove limitations as the definition of each water body is now purely geometric. We have incorporated a comprehensive review of the limitations and assumptions of the depth algorithm into Section 3 (lines 284-290).

Another point for the authors to consider, which deserves mention in the manuscript, is that this method will be unable to extract depth from lakes with floating ice cover (and hence will miss their deepest points).

We have clarified that water bodies with a floating ice cover effectively had their ice cover 'removed' and 'filled in' with water so the areas of these lakes are as accurate as possible. Pixels that had been 'filled in' due to ice cover were then prescribed the mean depth of their respective water bodies:

On lines 264-266, we have added: "To ensure that pixels with floating ice cover were still included in the analysis, we then used the 'imfill' function within MATLAB to classify any 'dry' pixels situated within a water body as water."

And on lines 311-313: "Pixels that had a floating ice cover and had been filled (see section 3.2) were assigned the mean depth of their respective water bodies, as it is not possible to calculate the depth of a pixel with an ice cover."

The authors use surface and ground surface air temperature from one weather station to assess meltwater changes against temperature changes. However, this is only at a single point location, and I suggest the authors could compare reanalysis or regional climate model temperature data over the whole ice shelf, or at least over a broader area, at least to see if a similar pattern is shown through the melt season. Such models are spatially distributed and provide daily outputs. I believe that some regional climate models have outputs at 5.5 km resolution over parts of Dronning

Maud Land. I leave it up to the authors to decide whether to include this additional analysis.

And minor comment: Line 314: See broader comments above.

We agree that this would be better, and we have therefore analysed data from "from an atmosphere-only regional climate CORDEX (COordinated Regional climate Downscaling Experiment) simulation of Antarctica using the limited-area configuration of Version 11.1 of the UK Met Office Unified Model (MetUM) for the period 2016-2017." Please see section 3.7 (lines 377-401) for a full explanation.

I would recommend that to strengthen the discussion in Section 5 the authors carry out flow routing analysis on a DEM in order to estimate the pathways in which surface meltwater would be routed. This would be particularly useful at end of third paragraph where the authors discuss the potential for excess meltwater export off the ice shelf.

We agree that this would be useful, and we attempted to carry out this analysis prior to initial submission. Unfortunately, the REMA data contains too many significant elevation errors and data gaps, meaning that flow routing analysis is extremely hard. 'Tidying up' the REMA data would be a large project in itself, and is something we think is beyond the scope of this current study.

The authors discuss the evolution of meltwater stored in the two largest meltwater systems. The meltwater volume loss from upstream lakes near the grounding line, and the gain in meltwater volume in these two large meltwater systems (WS and ES) through the melt season, should be more explicitly calculated in addition to the time series of total area and volume presented in Figure 6. This would help their discussion of lateral meltwater transfer across the shelf. A further optional suggestion is that the authors could include evidence that the firn contains shallow-sub- surface meltwater, e.g. visible as low backscatter in Sentinel 1 (Miles et al., 2017, Frontiers in Earth Science), which could aid their discussion of the likely processes responsible for meltwater transfer across the shelf.

We have included a new figure (Fig.8), which shows the volume and area of both the WS and ES throughout the melt season. This figure is discussed further in lines 498-502.

We have also included an additional new figure (Fig.11), which show an optical and a SAR image, this adds to our discussion (lines 583-597), and provides evidence of sub-surface meltwater storage within the firn.

Minor Comments

Line 30: Quantify how large (e.g. up to ~8/5 km long).

Corrected (Line 29)

Line 55: Consider also citing Bevan et al. (2017) here, who present four boreholes on Larsen C in addition to that reported by Hubbard et al. (2016).

Corrected (Line 58)

Line 103: 'flow velocities of around 100 m a^{-1}' – is this at the grounding line or near the calving front?

We realised that our previous sentence was vague. We have reworded this sentence to say the following (Lines 141-143): "Ice thickness ranges from 150 m at the calving front to ~ 700 m towards the ice shelf's grounding line in the southeast, and it exhibits flow velocities of around 20 m a^{-1} to 130 m a^{-1} (Horwath et al., 2006)."

We have not commented on the spatial arrangement of these flow velocities, as we see no obvious spatial gradient in Figure 7 of Horwath et al. (2006) (page 23):

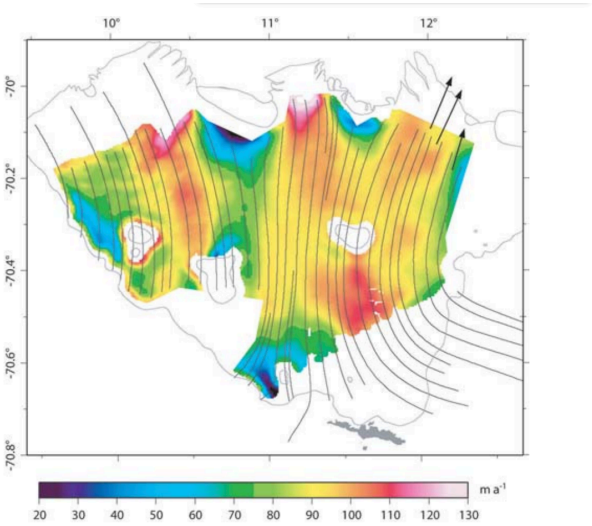

Fig. 7. Horizontal velocity field of Nivlisen derived from interferometric SAR processing. Black lines are flowlines deduced from the amplitude image and used to define the flow direction. Arrows show the GPS measurements used for the calibration.

Line 104: It would be helpful to label these regions on Figure 1, i.e. bare/blue ice area, Shirmacheroasen and the ice shelf itself. Red star is missing from Figure 1 inset.

Corrected (Figure 1)

Line 106: It would be useful to mention surface melt rates on the ice shelf in this section.

To the best of our knowledge, no surface melt rates have yet been measured on the Nivlisen Ice Shelf.

Line 117: Perhaps refer the reader to Figure 2 here.

Corrected (Line 164)

Line 127: Perhaps explain why you have chosen to conduct your analysis on a single melt season, and why this specific melt season has been chosen. You state yourselves in line 82 the importance of tracking meltwater evolution through entire summer melt seasons, so why not do it here? If this was because your focus was on testing FASTish over a relatively small area and time window, make this clearer. Or was this purely based on imagery availability?

We have justified this in lines 131-133 (Section 1) as we feel it is better placed here: "We then apply the FASTISh algorithm to the Nivlisen Ice Shelf, Antarctica, for the 2016-2017 melt season; the first full melt season to have data coverage over the ice shelf from both Landsat 8 and Sentinel-2."

Also, why not change 30th April 2017 to 24th March 2017, given this is the latest image you use.

Corrected (Line 173)

You also say you identified 12 scenes with 'minimal' cloud cover – did you select a specific % threshold?

And Line 166: As with Line 127, state the specific % cloud threshold used.

We visually picked images, as using a % threshold doesn't provide information on where in an image scene the cloud cover is. If there is 30 % cloud cover but off the ice shelf, we could still use the image. Whereas if there is 10 % cloud cover but over the main melt area, the image is not useful.

Line 141: How well does this cloud mask perform compared to other cloud masks? And why was this method used but then you computed a cloud mask using a different method for Sentinel 2 scenes?

We have clarified this in lines 202-204: "We found the 'simple cloud score algorithm' to be the most effective cloud masking method for Landsat 8 images, as it assesses each pixel using multiple criteria, making it more effective than any single band threshold."

And lines 229-232: "As the simple cloud score algorithm had not been adapted for application to S2 imagery at the time of writing, we computed a cloud mask for each image using a thresholding approach, whereby pixels were categorised as cloudy if the SWIR band value was > 10,000."

Line 184: I feel this is a bit vague – what was unsuccessful about this cloud masking approach? Were there false positives? Clouds not captured in the cloud mask? In addition, a little more detail might be added about how individual masks were manually created in these cases – were polygons manually digitised in GIS?

We have clarified these points in lines 235-238: "On two image dates (14th November 2016 and 25th February 2017), this cloud masking approach was not entirely

successful as not all clouds were fully masked. Additional individual masks were manually digitised in ArcGIS to ensure all clouds were masked for these images."

Line 209: Explain what a two-dimensional connective threshold is. Line 210: ≤ two pixels in total size, or in width? Same with Sentinel-2?

We have clarified these points in lines 259-264: "Having applied a 0.25 $NDWI_{ice}$ threshold to each image, the resulting water masks were filtered using a two-dimensional 8-connected threshold (i.e. grouping pixels if they were connected by their edges or corners) to identify each individual water body. Water bodies consisting of ≤ 2 pixels (Landsat 8) and ≤ 18 pixels (Sentinel-2), were removed to ensure only water bodies with an area ≥ 1,800 m^2 were assessed further."

Line 216: Rather than qualitative depth assessments, I would say that NDWI has been primarily used previously to derive water body extents and area, so would delete this second part of the sentence.

We agree, and have actually removed the beginning of this paragraph, as it wasn't very succinct (Line 270).

Line 239: The description of how Ad was calculated could be explained in slightly more detail.

Clarified in lines 296-298.

Line 244: Did all images include deep water? What range of R∞ values were used here? I believe Sneed and Hamilton (2011) conclude that optically-deep water is not required in every scene, and indeed Banwell et al. (2019) found a negligible difference of using a R∞ value of zero. I am interested whether you explored different values to see what difference it made.

Corrected (Lines 307-308): "For images that did not contain optically deep water, the R_∞ value was set to 0 (Banwell et al., 2019)."

Line 250: Figure 2 mentions the removal of negative depths from the area and depth matrix, yet this is not discussed in-text. Where did negative depths originate from, was this in the cases with floating ice on lake surfaces?

Clarified In lines 301-304: "In very rare cases, wet pixels within a water body could have a reflectance higher than the calculated A_d value, leading to negative water depths. All such pixels were removed from the area and depth matrix (Fig. 2)."

Line 261: I think the solidity score needs to be explained in greater detail here, i.e. that the score can range from 0 to 1 and denotes the proportion of pixels within the convex hull of the water body, with streams or linear lakes having a score closer to 0, and perfectly circular lakes having a score of 1.

Further clarification added (lines 322-329).

Line 276: Does FASTISh use the same minimum size threshold for tracking water bodies as in Williamson et al. (2018), i.e. 495 pixels (0.0495 km^2)? I couldn't see mention of this.

We track all the water bodies we identify. The threshold we apply for categorising water in a water body is already stated in Section 3.2 (lines 262-264).

Line 300: I think it needs to be made clear to the reader that a 'loss event' could either be a lake drainage or freeze-through. Given the previous sentence, one might assume this is just referring to lake drainage events only.

Sentence modified as suggested (lines 514-519): "Therefore, we used the calculated volume time series to identify water bodies in the 'always circular' category that lost > 80 % of their maximum volume over the full melt season, through either drainage or freeze through. We focus solely on the 'always circular' category to better understand the local loss of surface melt water in seemingly isolated and stationary water bodies. These events are referred to as 'loss events' hereafter." Please note we have moved this section into the results (Section 4.2.3) to improve the flow of the text.

Line 371: I assume the single 2 m data strip was also REMA, but maybe best to clarify.

Corrected (Line 364)

Line 331: I suggest you include total area of meltwater bodies in each time-step (i.e. when discussing Fig 4A-D), as well as mean and maximum water depths.

We agree, and also included total volume. These results are also shown in a new table (Table 1).

Line 355: Interesting that the mean and maximum depth at the peak of the melt season is lower than in early December, near the start of the melt season? Have the authors considered why this may be?

Yes, we have added an explanation for this in lines 480-486: "Between 17th December 2016 and 27th December 2016 'all water bodies' are characterised by 'deepening', as their total volume increases at a greater rate than their total area, and their mean depth increases (Tables 1 and 2, Fig. 7). Whereas between the 27th December and the 26th January, 'all water bodies' are characterised by 'spreading', as their total area increases at a faster rate than their total volume, and the mean water body depth decreases (Tables 1 and 2, Fig. 7)."

Line 423: Is it not possible to distinguish whether a water volume loss event is freeze-through or surface drainage? This would help quantify specifically how much meltwater is transferred across the ice shelf.

The temporal resolution of our data set (which is a factor of available cloud free imagery) is unfortunately not good enough to allow us to identify drainage events.

Line 520: I would suggest moving the last sentence of this paragraph (explaining FAC) to here.

We have changed our wording slightly, but the discussion around FAC is now at the end of the paragraph (lines 573-575).

Line 546: How did you derive albedo over water-free distal areas of the ice shelf?

We digitised a polygon over a water-free distal part of the ice shelf, and calculated the average albedo of the pixels within this polygon (lines 666-667).

Line 572: Consider changing this to 'Around the peak of the melt season (26th January 2017)'

Corrected (line 691).

Line 576: Perhaps consider adding a sentence or two about the wider application of your findings. For example, your mapped lake extents could be used as constraints in surface hydrology modelling simulations?

Lines 696-697: "Our findings could be useful in comparing to IceSat 2 derived lake depths, in addition to constraining future ice-shelf surface hydrology models."

Line 581: What about sharing your dataset publicly, i.e. lake extents containing attribute information of elevation, mean area, maximum area, mean depth, maximum depth.

Upon publication, we will upload our scripts to the Apollo Repository (Lines 701-703).

Line 817: Looking at your study area extent, it seems odd to include a couple of lakes above the grounding line but not all, when there are visibly quite a few more within the blue ice area above the grounding line which fall outside your study area boundary. Given these are probably 'feeder lakes' which help route meltwater to lakes and channels on the ice shelf, it seems incomplete not to track seasonal changes in their area and volume as well.

The study area extent was drawn to include the two feeder lakes identified by Kingslake et al. (2015). In hindsight, we should have extended it further back to consider other feeder lakes, but we were trying to keep the study area relatively small to reduce computer processing time. We are unfortunately unable to change this now as the full algorithm would have to be re-run. Despite this, we think the overall results and conclusions of the paper would remain largely unchanged if we did extend the study area further.

Line 839: Are the white stripes across the figure artefacts? Consider changing the colour ramp to make values easier to read, and outlining lakes in black for visibility.

We have modified the colour ramp. The white stripes were an odd artefact during image export, and have been removed. Unfortunately, we could not outline the lakes in black due to the format of the data. Please note this figure is now Figure 4.

Line 852: Again, the colours make visibility difficult. I struggle to pick out areas in the 'always a stream' category

Colour scheme has been amended (Fig 6)

Line 877: I find this figure slightly confusing, though perhaps I have mis-interpreted it – why is one bar not shown per individual date studied in the 2016-2017 melt season (i.e. only 8 bars are shown, not 11). Clarify caption to show that loss events record either lake drainage or freeze- through.

We only show 8 bars as no loss events were recorded on the other 3 dates. We have added the following statement to the caption (Figure 10): "A loss event is defined as a > 80 % loss in water body volume through either lake drainage or freeze-through."

Technical corrections

Line 23: inconsistent hyphenation of Landsat-8 and Sentinel-2 throughout the manuscript; please check throughout for consistency

Landsat 8 should not be hyphenated, whilst Sentinel-2 should be, we have checked this throughout the document.

Line 68: inconsistent hyphenation of sub-surface; please check throughout for consistency

Corrected

Line 69: re-order citations chronologically; please check and modify throughout

Corrected

Line 74: delete 'events'

Corrected (Line 83)

Line 76: delete comma after 'front'

Corrected (Line 84)

Line 81: change 'on' to 'in'

No longer necessary as wording altered to improve the flow of the text.

Line 102: is 'approximately' 123 km wide by 92 km long.

Corrected using '~' (line 139).

Line 161: 'change 'in' to 'into'

Corrected (Line 213)

Line 175: Change 'give' to 'produce'

Corrected (Line 226)

Line 201: Hyphenate 'water covered'

We have since removed this sentence.

Line 218: Delete 'different'

Corrected (Line 270), start of paragraph shortened.

Line 206: Change 'as' to 'because'

Corrected (Line 258)

Line 220: Correct (Philpot, 1989) to Philpot (1989)

Corrected (Line 272)

Line 294: Change 'track' to 'tracked'

Wording changed (line 511).

Line 393: Maximum should be ~3 x10^6 m^2, not 2.5 x10^7?

We are not sure where this confusion has come from, perhaps you were looking at the envelopment transitions in Figure 6 (now Fig. 7)? This is likely because we were not using an appropriate figure for Fig.7 (now Fig.8), which we have now changed based on your previous recommendations.

Line 426: change 'by' to 'on' (as this is showing loss events on that particular date rather than cumulative events, if I have understood correctly)

‘By’ is an appropriate word choice here, as the loss events did not occur on the single date, but rather ‘by’ this date.

Line 449: Change ‘weather’ to ‘temperature fluctuations’

Corrected (Line 549)

Line 467: New sentence after ‘bodies’. ‘We suggest this occurs when water ponds...’

This is no longer necessary as the text in this paragraph has been further edited.

Line 471: New sentence after ‘dam’. ‘Therefore, it is more likely to be the result...’

Corrected, with slightly different wording (Line 573).

Line 497: hyphenate snow/firn-covered

Corrected (Line 616)

Line 500: add ‘firn’ into ‘available pore space’

Wording since altered .

Line 547: hyphenate ‘large scale’

Corrected (throughout text)

Line 863: Western and Eastern System are the wrong way round in the figure caption. Wrong dates in legends?

Based on your recommendations (above) we have removed this figure and the text relating to it, replacing it with a more suitable figure showing the volume and area of the ES and WS (Fig. 8).

Response to Reviewer Comments – Reviewer 2

This manuscript describes the evolution of surface meltwater on the Nivlisen Ice Shelf in Antarctica during the 2016-2017 melt season. The authors describe in detail their adaptation of the FAST algorithm for tracking water on ice shelves, and apply the method to two optical satellite datasets. They develop four categories of ice-shelf water bodies, and use them to discuss water transport across the Nivlisen Ice Shelf. Two main systems emerge on the ice shelf along linear surface depressions as the surface hydrology system transitions from isolated lakes to a connected network.

As explained in the introduction, ice-shelf surface hydrology is a critical component of ice-shelf stability, and thus important in predictions of ice-sheet mass loss. Being able to map and analyse the development of ice-shelf surface hydrology is important for understanding how future warming and subsequent ice-shelf melting will influence ice shelf behaviour. There is a significant gap in our knowledge of water transport across ice shelves, and the goals of this manuscript are both timely and within the scope of TC. In general this manuscript is well written and should be published in TC with some revisions applied. The topic of ice-shelf meltwater transport is important, and the results of this study will certainly be of interest to the TC audience.

We thank Reviewer 2 for their positive and constructive overview and further feedback on this paper.

Major Comments:

This manuscript builds on previously developed tools (water-tracking algorithms, band ratios, etc) and applies them to an ice-shelf whose surface hydrology has not to my knowledge been analysed in detail. The authors have adapted these methods and tools to suit ice shelves, and combined this algorithm with previously validated methods of water volume retrieval from satellite imagery. However, the authors do not clarify why the FAST algorithm is not suitable for use on ice shelves and do not explain the differences between the FASTER algorithm and their new FASTISh.

Additional major comment: *In terms of the methods, providing context for the FASTISh algorithm would go a long way. A lot of time is spent in the beginning discussing a method that is at this point standard in ice-shelf/ice-sheet hydrology, and it's not clear how FASTISh differs from FAST.*

Additional minor comment: *Line 92: Why is it necessary to produce FASTISh? It would be very helpful to include a description of FAST, highlighting its strengths and weaknesses.*

We have provided justifications for adapting FASTER for application to Antarctic ice shelves in lines 100-117, we have also made the differences between the FASTER and FASTISh algorithms clearer (lines 121-133).

The authors clearly demonstrate an evolving meltwater system on the Nivlisen Ice Shelf, and clearly describe why these observations are important for ice-shelf

stability. However, the conclusions could use some clarification and possibly additional analysis. First of all, the difference between a meltwater lake and a stream is defined here only geometrically. Streams and rivers are defined by water flow, but the definition used here does not include a water flow condition. Rivers and streams described here could technically be linear lakes that fill up from percolation through the firn. The authors seem to support this, since they describe two mechanisms for water transport 1) movement through firn and 2) movement via overtopping lakes, but then claim there is no evidence of overtopping lakes. There is not sufficient data or analysis to confirm water is flowing in these features precisely because water transport in the firn cannot be tracked from optical satellite imagery.

And a minor comment: Line 357-358: I am now getting confused between lakes and streams- are the two "large streams" just linear lakes? Your distinction between the two is only geometric. It is not clear that water flows in these water bodies the way water flows in streams. I am convinced water is transported, but I don't think there is clear evidence for how. Except that you later say you have no evidence for water overtopping lakes, which makes me think you are concluding most water moves through firn.

Based on our current level of analysis, we now agree that it is not possible to confidently categorise water bodies as lakes or streams. We have therefore re-named our categories to purely reflect the geometry of the water bodies, and water bodies are classified as either circular or linear. These adjustments have been made where appropriate throughout the manuscript. We also argue throughout the discussion for the lateral movement of water through the firn pack (e.g lines 583-597).

We have further clarified our argument for overtopping of lakes in the discussion. We DO argue for potential overtopping of water bodies (see lines 568-571), but we argue that the two large linear systems (the ES and the WS) do not develop through overtopping a dam, rather they just follow their downward sloping profiles as the melt season progresses (see lines 571-575 and 556-558).

Satellite radar could be used to track melt in the upper firn layers and might provide insights into exactly how water is moving. Additionally, the authors have not explained where firn is located on the ice shelf or how it is detected. I think it was visually identified. That should be briefly described and indicated on one or more maps (along with blue ice areas).

We have incorporated a Sentinel-1 SAR image into our discussion and into a new figure (Figure 11). We have used this to further our argument for lateral water transfer across the ice shelf through the ES and WS. This figure also provides evidence for both the ES and WS infiltrating into the firn pack (lines 583-597). We have also added a description of where we believe the firn to be located in Section 2 (lines 145-147).

The connection between temperature and surface hydrology development could be enhanced by including data from a climate model that covers the entire ice shelf as opposed to a single weather station. The development of air and ground

temperatures could be tracked through space and time and then be compared to the development of the surface hydrology system that the authors already quantified.

And: *Also I think a single point of temperature is insufficient for this analysis. It would be useful to see modeled (maybe RACMO) temperature and energy balance across the extent of the surface hydrology system.*

We agree with this, and we have therefore analysed air temperatures "from an atmosphere-only regional climate CORDEX (COordinated Regional climate Downscaling Experiment) simulation of Antarctica using the limited-area configuration of Version 11.1 of the UK Met Office Unified Model (MetUM) for the period 2016-2017." Please see section 3.7 for a full explanation.

We have, however, not looked at spatial gradients in the climate data, as we believe this is something that is beyond the scope of this current study.

The general structure of the manuscript could be improved by including some of the more important conclusions and implications in the abstract and introduction. For example, the comparison to the surface lakes of Larsen B in the discussion could be highlighted to provide some motivation for the study, as opposed to limiting the goal of the study to developing an algorithm and tracking water on one ice shelf.

We agree with this comment and have made adjustments in the abstract (lines 29-33), and introduction (lines 63-67).

Some more context for the Nivlisen Ice Shelf would be helpful in Section 2.

We have added more context for the Nivlisen Ice Shelf, and have described the blue ice extent and firn extent in greater detail (lines 145-147), we have also expanded our justifications for selecting Nivlisen Ice Shelf as the study area (lines 150-157).

Figures:

Titles would help the reader interpret figures more easily.

Corrected throughout

Figure 1. Add coordinates to Nivlisen map, include location of weather station. Annotate blue ice areas, water bodies and firn extent. The caption refers to a red star to locate the Nivlisen Ice Shelf, but I don't see it. Also, is this image mosaicked? From the description of data preparation, it seems like the entire ice shelf cannot be captured by a single Landsat scene, and that pairs of scenes were mosaicked.

We have added blue ice areas and co-ordinates to Figure 1. To clarify the firn extent on the ice shelf we have added this statement to Section 2, as it would be clearer than labelling the map (lines 145-147): "Beyond this blue ice region, towards the north, the ice shelf transitions into an accumulation zone as the firn layer thickens (Horwath et al., 2006)."

The weather station data is no longer used for this study, so we have not added this location. Given the amount of information already on the figure, we have decided not to label the water bodies, as it would be difficult to label the full extent of all water here clearly

We have also clarified that the image is mosaicked (line 1000).

Figure 2. This is a nice workflow diagram. One very detail-oriented comment: It is a little confusing to have "Cloud Mask" in an input, and then the next line be the "Apply Cloud Mask" processes in the same workflow. From my understanding of the workflow, cloud masks are generated from a separate workflow followed in Google Earth Engine and are then an output of that workflow. Maybe delete the "Cloud Mask" input from the top.

Corrected (Fig.2).

Figure 3. Include the paths of the DEM that were extracted and shown in Figure 8. Consider combining this figure with Figure 8 and maybe Figure 7. It would be nice to have an "elevation figure" to synthesize everything.

We have removed Figure 7 based on recommendations made by Reviewer 1, and replaced it with a different Figure (now Figure 8). We would also like to keep Figures 3 (now Fig.4) and 8 (now Fig.9) separate, as they draw upon two different types of REMA data. Figure 3 (4) shows the 8 m mosaicked data product, whilst Figure 8 (9) utilises the 2 m data strips. The paths extracted for the DEM in Figure 8 are shown in Supplementary Figure 5.

Figure 4. This shows the water transport really nicely. Consider having the scale bar on only one image so that the eye can focus more on the water. Also, consider making the color of lakes and streams more distinct- it is hard to distinguish in print and only slightly easier on screen. Also, the text references streams a and b on line 343, but I think you should keep names and labels consistent. Label them here, since it is the first time we see the hydrologic system. Maybe add labels to row D.

All suggested changes made. However, we have continued to label the 'streams' (now called linear water bodies) as 'a' and 'b' as at this point in the results, as we have not introduced the ES and WS, which are products of the tracking results (which are not introduced until section 4.2). Please note this is now Figure 5.

Figure 5. Great figure! Move the WS and ES labels so they don't overlap the nice masks. Is the basemap Landsat? Include that in the caption. Is it necessary to include a category for water that isn't mapped if the background shows a satellite image? It makes me want to look for what features with a gray outline.

We have moved the labels, and changed the colours for each category to make the figure clearer and to reflect the changes made to Figure 5. We have also removed the category for water that isn't mapped, and have clarified where the base image is

from in the caption: “Base image aquired by Sentinel-2 on 26th January 2017” (Line 1049). Please note this is now Figure 6.

Figure 6. Get rid of white space after 01-04-17 since nothing is plotted there.

Corrected. Please note this is now Fig.7. We have also adjusted the line colours to reflect the changes made in Figures 4 (now Fig 5) and 5 (now Fig.6).

Actually, if I’m correct in this interpretation, it seems like this figure shows a period of water deepening– in the All Water Bodies and Envelopment Transitions categories, the volume increases at a greater rate than the area from ~ 01-12-16 to 01-02-17.

This is roughly correct, we have added the following statement to section 4.2.1 (lines 480-486): “Between 17th December 2016 and 27th December 2016 ‘all water bodies’ are characterised by ‘deepening’, as their total volume increases at a greater rate than their total area, and their mean depth increases (Tables 1 and 2, Fig. 7). Whereas between the 27th December and the 26th January, ‘all water bodies’ are characterised by ‘spreading’, as their total area increases at a faster rate than their total volume, and the mean water body depth decreases (Tables 1 and 2, Fig. 7).”

Figure 7. This figure basically tells me that water flows downhill. This is very encouraging, but I think that’s communicated in the combination of Figures 3 and 4.

We have removed this figure and replaced with another figure to address a comment from Reviewer 1 (please note this is now Figure 8).

Specific comments:

Line 1: change “stored” to “can form”

Wording adapted further to: “Surface meltwater on ice shelves can exist as slush, it can pond in lakes or crevasses, or it can flow in surface streams and rivers.” (Lines 15-16).

Line 31: I don’t think it’s clear that water transfer is “facilitated by two large surface streams.” In fact, the discussion seems to indicate lateral transport of water through firn.

We have reworded this to: “At this time, 63% of the total volume is held within two linear surface meltwater systems, which are up to 27 km long, are orientated along the ice shelf’s north-south axis, and follow the surface slope. Over the course of the melt season, they appear to migrate away from the grounding line, while growing in size and enveloping smaller water bodies. This suggests there is large-scale lateral water transfer through the surface meltwater system and the firn pack towards the ice-shelf front during the summer.” (Lines 28-33).

Line 80: I agree it is important to assess the variability of ice-shelf surface hydrology over the course of a melt season, but the year-to-year change is also critical. As just

one example, the Nansen River does not form every year (Bell et al. 2017). If meltwater transport is such an important part of ice-shelf stability, then its variable behaviour must be important, too. What if water didn't move across Nivlisen one year?

We have appended 'and across multiple melt seasons' to this sentence (line 90).

Line 98: In general I would like more description of the ice shelf here. A discussion of the firn would be useful.

We have added much more detail to section 2 (lines 137-157), including a description of the firn extent (lines 145-147).

Line 103: Be more specific about where the ice thickness reaches 700 m. Is 700 m a grounding line thickness? Taking a look at Horwath et al., referred to in the text, it looks like it might be.

Yes, it is towards the grounding line. Clarified on lines 139-141: "Ice thickness ranges from 150 m at the calving front to ~ 700 m towards the ice shelf's grounding line in the southeast, and it exhibits flow velocities of around 20 m a^{-1} to 130 m a^{-1} (Horwath et al., 2006)."

Line 105: It would be helpful to include a reference to Fig. 1 here with some annotations provided.

Corrected (Line 145)

Line 110 (Study Area in general): Discuss meltwater features in more detail than "meltwater features show changes over time." Kinglsake et al. 2015 specifically say that lakes drain on the Nivlisen Ice Shelf. You may disagree with the classification of the meltwater identified by Kingslake et al. 2015 – the images there look like what you call an "envelope transition." However, "changes over time" doesn't communicate enough information to the reader. This description could include basic information from your analysis, too. Knowing up front how large the extent of melting is compared to the total area of the ice shelf, for example, would be helpful in orienting the reader. Also including some basic climate information would be good, especially since you talk about temperature data later.

We have discussed the findings of Kingslake et al. (2015) in more detail (lines 153-155): "these meltwater features have shown significant development over a melt season, as source lakes upstream of the grounding line appeared to drain laterally, rapidly flooding large areas of the ice shelf (Kingslake et al., 2015)"

We have also incorporated basic climate and melt extent information in lines 147-149: "In the 2016-2017 melt season, air temperatures on the Nivlisen Ice Shelf ranged between ~ -25°C and 2°C, and 1.6 % of the study area occupied by a surface water body at least once during this time."

Line 139: Converting from DN to TOA values is important for analysing spectra anywhere, not just at high latitudes.

This is true, but typically landsat scenes are corrected for TOA using a single solar angle over the full image scene, here, we correct each pixel with individual solar angles, as at high latitudes the solar angle can vary significantly over a full image scene. We have clarified this within the text (lines 179-187):

"Typically, Landsat scenes are converted to TOA reflectance values using a single solar angle over the whole image scene. However, here we correct each pixel for the specific solar illumination angle, based on metadata stored in the .ANG file, and using the 'Solar and View Angle Generation Algorithm' provided by NASA (https://landsat.usgs.gov/sites/default/files/documents/LSDS-1928_L8-OLI-TIRS_Solar-View-Angle-Generation_ADD.pdf). Converting from DN to TOA values on a per-pixel basis is imperative when mosaicking and comparing images obtained at high latitudes, as the solar angle at the time of acquisition can vary significantly across each scene due to the large change in longitude."

Line 156: I appreciate that clipping each scene to the same extent is a required step in the algorithm, but I don't understand the reason. Although you say "when comparing images," but you can compare scenes that have overlapping areas but not the same extent. This makes me think there is some other requirement that you haven't mentioned.

We have clarified this in lines 206-209:

"Clipping each scene to the same extent is required when comparing images through the FASTISh algorithm, as tracking individual features over time requires images with a consistent spatial reference frame to determine the location of each water body."

Line 168: It might be good to describe bands in terms of their spectral range rather than colour, since you are using imagery from two different platforms. Clearly this is not critical, just a thought.

For simplicity for the reader and easy comparison between the two platforms, we would like to keep these as colours.

Line 171: The division by a "quantification value" comes out of nowhere. Is there a paper you could cite that explains this as a part of data processing? I would delete "expected" since it can imply that something is wrong with Sentinel-2, when it seems like it's just a convention of how they deliver their data. I haven't worked much with Sentinel-2, however, so if this really is an unexpected discrepancy then ignore my suggestion.

We have deleted 'expected' as suggested (line 222), and have included a supporting citation (Traganos et al., 2018) (line 223-224).

Line 178: Is the thresholding approach the same as before?

No, we have clarified this by adjusting our wording (Lines 229-232): “As the simple cloud score algorithm had not been adapted for application to S2 imagery at the time of writing, we computed a cloud mask for each image using a thresholding approach, whereby pixels were categorised as cloudy if the SWIR band value was > 10,000.”

Line 179: How can a value exceed 10,000 if all bands were divided by 10,000?

We only converted bands 2,3,4 to the 0-1 range as these were used in main area and depth analysis. We did not convert band 11 as it seemed unnecessary. We have better clarified this in lines (224-226).

Line 233: While I know it is correct to say that errors in lake depth estimates have been calculated as zero (Pope et al. 2016), I think it is misleading to have this be the only mention of error about this method. To a reader who isn't already familiar with this method, the claim that error is zero will be shocking, and probably lead to skepticism. I think that if you are going to describe the method to help the reader understand what you did, it is important to give a little bit more detail about the sensitivity to A and g, the dependence of the band chosen, and that physical qualities of the system are known (water column attenuation, surface roughess of the lake, etc.)

We agree with this, and we received a very similar comment from Reviewer 1. We have incorporated a comprehensive review of the limitations and assumptions of the depth algorithm into Section 3 (lines 283-290).

Line 265: I'd really like to see a figure of the thresholds and different water body shapes. I think it would help me understand the categories you introduce in section 3.5.

We have included a new figure (Fig.3), showing three of the thresholds tested. This is clearer than showing every threshold tested.

Line 286: There should definitely be a figure for this. It could be Figure 5, but I would almost prefer a zoomed-in high detail of an area with one of each type.

We feel that Figure 5 (now Figure 6) really does do this, we have made the colour scheme clearer. The addition of the new Figure 3 will also help to show how we selected linear and circular water bodies, which feed into the final tracked water body categories.

Line 308: Is the figure for this Fig. 7? If so, refer to it. But also, be clear about which water bodies. I was expecting an elevation profile with different colours representing your four water body categories, whereas Fig. 7 shows the Eastern and Western Systems.

We have clarified this (lines 370-373): “In addition, a single 2 m REMA data strip from 31st January 2016 was used to extract the elevation profiles along two tracked water bodies, the Eastern System and the Western System, which are introduced in section

4.2.2 ” However, we do not want to refer to the Figure (now Fig.9) at this point in the paper, as it will introduce results too early in the paper.

Section 3.7: Plot this on a map- I can't figure out where it is!

As we are now using modelled climate data rather than weather station data, this is no longer necessary.

Line 326 and Section 4.1: Give a general synthesis. Instead of only having four paragraphs that describe the observations, tell the reader the overall trend. I can't really grab on to a take-away message the way it is written.

We have synthesised the main message in an 'introductory' paragraph to this section (lines 414-418):

"The seasonal evolution of meltwater bodies during the 2016-2017 summer is shown in Figure 5. The surface meltwater system transitions from a series of small isolated water bodies clustered towards the grounding line (Fig 5A), to a connected system dominated by two linear water bodies with a length of (a) ~ 20.5 km and (b) ~ 16.9 km that propagate towards the ice-shelf front (Fig 5D)."

We have then improved the flow of the following text (lines 420-458).

Line 328-29: Ice shelves are flat places- what does relatively flat mean and how do you know how thin the winter snow cover is?

We have adjusted the text (Lines 420-422) to read as follows: On 11th December 2016, few meltwater bodies exist, and they are predominantly clustered within the blue ice region towards the grounding line in the south-west (Fig 5.A).

Line 343-344: Refer to Fig. 5.

We think it is actually better to refer to Figure 4 (now Figure 5) rather than Figure 5 (now Figure 6) here.

Line 353: Again, how do you know the extent of the firn? If it is visually identified, consider digitizing it. I'd be curious to see how the firn extent changes as the system evolves, especially given your discussion section.

The firn extent covers the ice shelf area north of the blue ice region. We have clearly labelled the blue ice region in Fig.1 and have also added a description of the firn extent into Section 2 (lines 145-147).

Line 385-387: The FASTISh algorithm itself does not produce a time series of water body properties- it only does you have used it on a time series of images.

We have reworded this sentence to: "In addition to quantifying total surface water area and volume for each of the four water body categories (Fig. 7, Table 2), the

FASTISh algorithm also tracks changes in the area and volume of *individual* water bodies." (Lines 490-492).

Line 392-397: While you refer to Fig. 7 for this, that figure only shows migration to lower elevations, not lower latitudes. I am not sure what trends you refer to in section 4.1 – rewriting that section to include a general point would help. Then refer to it here by saying "In line with the XYZ trends described in section 4.1. . ..."

We did not write this section well previously, we have since removed and replaced Figure 7 (now Figure 8) in response to a combination of suggestions from both reviewers. Figure 7 (now Figure 8) no longer shows the elevation profile of the ES and WS, but instead it shows the total area and volume of the ES and WS. This is described in lines 498-502. We then describe the surface slope followed by both systems (lines 502-507), with reference to Figure 9.

Line 399: I got confused between the Eastern System and Western System and the water body categories. When I looked at Fig. 7 I was expecting to see the four categories, since the title of the section is "Tracking Individual Water Bodies." Why have you not done this? Is it because most of the water is in the ES and WS? It would make sense to focus on these two, given that there is also migration of both systems. But I think that needs to be clarified in the text. It is even more confusing in the rest of the paragraph because on line 404 you say "most of the surface water" and it's not clear if you mean "most of the surface water in each meltwater system" (and I don't even know which meltwater system it is, east or west?) or if you mean "most of the surface water on the ice shelf".

Figure 6 (now Figure 7) shows the time series for the four distinct categories. But, yes, we focus Figure 7 (now Figure 8) on the ES and WS as they hold the majority of the surface melt at the peak of the melt season. We have clarified in that we are only referring to the ES and WS within section 4.2.2 (lines 495-496).

We no longer refer to 'most of the surface water' – as this section has been largely re-written to reflect the changes made to Fig.7 (now Fig.8).

Line 418-419: I'm not sure this sentence matters. What is rhythmic variance? What do these properties mean for the surface water?

We have removed this sentence.

Line 448: You say surface water area and volume correspond with rising temperatures, but Fig. 9 shows volume loss is associated with temperature increase, and only in the category of "always a lake" when most of the water is contained in the ES and WS. It would be helpful to include a figure showing what is claimed on line 453 "As temperatures rise and surface water bodies increase in area and volume. . .." It seems like the point you are trying to make in this section is that temperature controls the evolution of the system, so showing the decreasing lakes with increasing envelopment transition might make that clearer. Although later it seems like you are claiming the opposite.

And *Line 508-526: It seems like now you are saying temperature does not control the evolution of the surface hydrology system. Earlier it seemed like you were saying the opposite.*

We have modified Fig.9 (now Fig.10) into 2 panels. Panel 'a' shows the temperature data and panel 'b' shows the volume loss from circular water bodies as well as a plot of the total surface water volume observed on each date.

"The loss of 1.5 x 10^7 m^3 of surface water from the circular water bodies by 27th December 2017 follows sustained relatively warmer atmospheric conditions since the beginning of December 2017 (Fig. 10), and coincides with an increase in the total surface water volume on the ice shelf (Fig 10b). In particular, we see an increase in the volume of water held within the enveloping water bodies, which continues to increase up to a maximum of 4.5 x 10^7 m^3 on 26th January 2017 (Fig. 7). It is likely, therefore, that the loss of water from circular water bodies at this early stage in the melt season signifies the lateral transfer of water away from the small 'isolated' bodies near the grounding line into the large enveloping water bodies which hold and transport the surface meltwater across the ice shelf to more distal regions." (Lines 628-636).

Line 463: How do you know water is flowing along linear depressions as opposed to those depressions being filled from the sides due to transport in the firn? Especially since you mention on line 470-472 that the growth of ES and WS are more likely to be fed by increased meltwater production and movement through firn. In general, I think you argue well for meltwater transport through firn. I would highlight that, but it would require a little more discussion and analysis of how you track firn on the surface.

We have changed our statement (lines 563-564) to say: "This is because these systems facilitate large-scale transfer of water across the shelf, as water ponds within linear depressions."

We have clarified the extent of the firn in Section 2 of the paper.

Line 464-468: You have not demonstrated that the ES and WS are "fed by smaller surface lakes and streams both above and below the grounding line."

We agree, so have removed this statement.

Line 470-472: Is it really possible to infer this when there are no images between Dec. 27th and Jan 26th? I assume that evidence of a "lip" would be the development of a stream forming out of a lake. How do you know this didn't happen? Also, refer to Fig. 4 here.

From looking at the DEM data available to use, we see no significant lip/ dam blocking the flow of water in either the ES or WS at these points.

Line 480-482: You claim it is possible that meltwater could be transported to the front of the ice shelf in the future. That would require water to organize in a river that can

flow off the ice-shelf edge (unless there is some meltwater evacuation through firn that I don't know about, but that's another can of worms). You could potentially demonstrate this by assuming at some point the firn will saturate and water will follow surface depressions (you have already argued that this is happening). You could perform a water routing analysis on the full DEM, or at least see if you can visually identify linear surface depressions out to the edge of the shelf.

We have expanded our argument slightly within lines 603-605, which builds upon our previous discussion.

We agree that flow routing analysis would be useful, and we attempted to carry out this analysis prior to initial submission. Unfortunately, the REMA data contains too many significant elevation errors and data gaps, meaning that flow routing analysis is extremely hard. 'Tidying up' the REMA data would be a large project in itself, and is something we think is beyond the scope of this current study. Visually, we can't yet see linear surface depressions propagating out towards the ice shelf edge.

Line 488-501: "The relatively extensive snow and firn cover . . .likely prevents the development of. . .meltwater. . .on the Larsen B." This is a very important distinction that I think you should highlight (maybe include it in the abstract and allude to it in the introduction?). This is definitely an important conclusion, because it defines a type of meltwater type and evolution that stands in contrast to the "ponds break ice shelves" style of meltwater without needing to remove water.

We have altered and clarified our argument slightly here (lines 617-621): "The development of these large, linear water bodies is likely facilitated by topography, and allows the transfer of summer meltwater towards the ice-shelf front. This large scale lateral transfer of meltwater is further facilitated as the ES and WS develop over frozen meltwater paths from previous years (Kingslake et al., 2015)."

Please note we do still discuss the importance of the firn layer in lines 583-597 and in lines 573-575.

*Line 515-518: Earlier you said that the transfer of water was *not* due to overtopping of surface lakes.*

Not quite, we argue that the progression of the ES and WS did not result from the overtopping of a topographic lip. However, this statement only applies to the ES and WS. We have clarified this in lines 565-575.

Line 530-552: What are the implications for the stability of Nivlisen? Could you tie your analysis more explicitly to our general understanding of ice-shelf stability? Your refreezing calculation is really interesting, but has nothing to do with the rest of the paper. It makes me again want to know more about firn on this ice shelf.

Beyond our discussion within Section 5.3 on the significance of ponding vs rivers exporting water off the ice shelf edge, and latent heat release upon re-freezing, we cannot think of much we can add without incorporating further analysis beyond the scope of the paper.

Line 558-576: I would lead with the conclusions you reach about the ice shelf, not with a description of your method, and also include a summary of the implications of your analysis.

We've kept the general structure of the conclusions as we think it's good to briefly summarise the methodology as well as the results. But we are happy to restructure it if the editor/journal style requires us to.

Line 570: Again, how do you know there is a thin snow band and firn pack?

This was a generous assumption as we likely can't differentiate between the snow and the firn, we have therefore removed this statement.

Technical comments

Line 20: hyphenate "ice-shelf"
Line 59: hyphenate "ice-shelf"
Line 76: hyphenate "ice-shelf"
Line 548: hyphenate "ice-shelf"

Corrected where appropriate throughout text.

Line 210: change "two" to "2" since it follows a mathematical symbol, even though it is a number less than ten.

Corrected (Line 262)

Line 294: "identified and tracked"

Wording changed, no longer applicable.

Line 306-307: Spell out acronyms when you use them for the first time REMA and DEM.

Corrected (Lines 368-369)

References

Horwath, M., Dietrich, R., Baessler, M., Nixdorf, U., Steinhage, D., Fritzsche, D., Damm, V. and Reitmayr, G.: Nivlisen, an Antarctic ice shelf in Dronning Maud Land: Geodetic-glaciological results from a combined analysis of ice thickness, ice surface height and ice-flow observations, J. Glaciol., 52(176), 17–30, doi:10.3189/172756506781828953, 2006

Lateral meltwater transfer across an Antarctic ice shelf

Rebecca Dell[1,2], Neil Arnold[1], Ian Willis[1], Alison Banwell[3,1], Andrew Williamson[1], Hamish Pritchard[2], and Andrew Orr[2]

[1]Scott Polar Research Institute, Lensfield Road, Cambridge, CB2 1ER, UK
[2]British Antarctic Survey, High Cross, Madingley Road, Cambridge, CB3 0ET, UK
[3]Cooperative Institute for Research in Environmental Sciences, University of Colorado Boulder, Boulder, CO, 80309, USA
copernicus-publications
Correspondence to: Rebecca Dell (rld46@cam.ac.uk)

Abstract

Surface meltwater on ice shelves can exist as slush, it can pond in lakes or crevasses, or it can flow in surface streams and rivers. The collapse of the Larsen B Ice Shelf in 2002 has been attributed to the sudden drainage of ~3000 surface lakes, and has highlighted the potential for surface water to cause ice-shelf instability. Surface meltwater systems have been identified across numerous Antarctic ice shelves, although the extent to which these systems impact ice-shelf instability is poorly constrained. To better understand the role of surface meltwater systems on ice shelves, it is important to track their seasonal development, monitoring the fluctuations in surface water volume and the transfer of water across ice-shelf surfaces. Here, we use Landsat 8 and Sentinel-2 imagery to track surface meltwater across the Nivlisen Ice Shelf in the 2016-2017 melt season. We develop the Fully Automated Supraglacial-Water Tracking algorithm for Ice Shelves (FASTISh) and use it to identify and track the development of 1598 water bodies, which we classify as either circular or linear. The total volume of surface meltwater peaks on 26th January 2017 at 5.5 x 10^7 m^3. At this time, 63% of the total volume is held within two linear surface meltwater systems, which are up to 27 km long, are orientated along the ice shelf's north-south axis, and follow the surface slope. Over the course of the melt season, they appear to migrate away from the grounding line, while growing in size and enveloping smaller water bodies. This suggests there is large-scale lateral water transfer through the surface meltwater system and the firn pack towards the ice-shelf front during the summer. ~~, thereby facilitating the large scale transfer of water towards the ice shelf front.~~

1 Introduction

The total mass loss from Antarctica has increased from 40 ± 9 Gt/y in 1979–1990 to 252 ± 26 Gt/y in 2009–2017, providing a cumulative contribution to sea-level rise of 14.0 ± 2.0 mm since 1979 (Rignot et al., 2019). Mass loss from Antarctica will likely increase in the near future due, at least in part, to the shrinkage and thinning of some of its ice shelves (Kuipers Munneke et al., 2014; DeConto and Pollard, 2016; Siegert et al., 2019) and the associated acceleration of inland ice across the grounding lines (Fürst et al., 2016; Gudmundsson et al., 2019). Seven out of 12 ice-shelves that bordered the Antarctic Peninsula have collapsed

in the last 50 years (Cook and Vaughan, 2010). One of the most notable events was the February-March 2002 collapse of Larsen B, leading to both an instantaneous and a longer term speedup of the glaciers previously buttressed by the ice shelf (Scambos et al., 2004; Wuite et al., 2015; De Rydt et al., 2015), and resulting in their increased contribution to sea level rise (Rignot et al., 2004).

The unforeseen catastrophic disintegration of Larsen B highlighted the unpredictable nature of ice-shelf collapse, and prompted a search for the causes of ice-shelf instability. Current understanding of the factors causing ice-shelf instability stems from the very limited number of airborne and satellite observations prior to and following collapse events (e.g. Glasser and Scambos, 2008; Scambos et al. 2009; Banwell et al., 2014, Leeson et al., 2020), numerical modelling (e.g. Vieli et al. 2006, Banwell et al. 2013, Banwell and MacAyeal, 2015), and the few in-situ measurements investigating recent and current ice-shelf processes (e.g. Hubbard et al. 2016; Bevan et al., 2017; Banwell et al. 2019). It has been suggested that the chain reaction drainage of ~3000 surface meltwater lakes, which covered 5.3% of the total ice-shelf area and had a mean depth of 0.82 m (Banwell et al., 2014), may have triggered the near-instantaneous break-up of Larsen B (Banwell et al., 2013; Robel and Banwell, 2019), highlighting the potential importance of surface hydrology for ice-shelf instability. The formation of these ~3000 surface lakes has been attributed to the saturation of the ice shelf's firn layer, making it impermeable (Kupiers Munneke et al., 2014; Leeson et al., 2020). Given this possible role of surface water on ice-shelf stability, it is important to monitor changes in the area and volume of surface meltwater systems across ice shelves, and compare any trends with those observed at Larsen B prior to its collapse.

Kingslake et al. (2017) identified numerous pervasive surface meltwater systems across many of Antarctica's ice shelves. Meltwater production is often highest around grounding lines, driven by high net shortwave radiation associated with low albedo blue ice areas, high net longwave radiation around nunataks, and high sensible heat transfer from adiabatic warming of katabatic (Lenaerts et al., 2017) and foehn winds (Bell et al., 2018; Datta et al., 2019). Ice-shelf hydrological systems may then take several forms as meltwater may: (i) form surface streams and flow downslope (e.g. Liston and Winther, 2005; Bell et al. 2017); (ii) collect in surface lakes (e.g. Langley et al. 2016); (iii) percolate into the sub-surface and refreeze (Luckman et al., 2014; Hubbard et al., 2016; Bevan et al., 2017); (iv) percolate into the subsurface and flow laterally (Winther et al., 1996; Liston et al., 1999); or (v) percolate into the subsurface and form sub-surface lakes and reservoirs (e.g. Lenaerts et al. 2017). Despite the identification of pervasive meltwater systems, very little is known about their spatial and temporal evolution, both within and between melt seasons. Furthermore, while surface water ponding and the formation of lakes have been implicated in past ice-shelf collapse (Scambos et al., 2003; Banwell et al., 2013), the formation of surface water streams that route water quickly to the ice-shelf front may not necessarily cause instability but rather mitigate against potential surface meltwater-driven collapse (Bell et al., 2017; Banwell, 2017). Thus, whether future projected increased surface melt on ice shelves forms lakes or flows rapidly to the ocean via streams has important implications for future ice-shelf stability and potential collapse. To better understand the behavior of surface meltwater lakes and

streams , it is important to investigate their spatial and temporal evolution across entire ice shelves through entire summer melt seasons and over multiple melt seasons.

In this paper, our objective is to develop a tool that can identify surface meltwater bodies on Antarctic ice shelves and track their evolution over time. We build on the work of Pope et al. (2016) and Selmes et al. (2011, 2013) and especially Williamson et al. (2017; 2018a), who developed and used the FAST algorithm for tracking lakes on the Greenland Ice Sheet (GrIS) using MODIS imagery. More specifically, we have adapted the FASTER algorithm of Williamson, et al. (2018b) and Miles et al. (2017), who adapted the FAST method to track GrIS lakes from the higher resolution Landsat 8 and Sentinel-1 and -2 imagery.

These previous methods need adapting for application on Antarctic ice shelves for three main reasons. First, to account for the observed differences in the geometry of surface meltwater bodies compared to those on the GrIS. Second, to recognise the marked geometry changes that occur over time on Antarctic ice shelves, including the joining of water bodies and the enveloping of some water bodies by others. Third, to identify the apparent transfer of surface melt water over large distances across ice shelves. In Greenland, the majority of surface water bodies form in surface depressions that result from undulations in the bedrock topography and ice flow (Echelmeyer et al., 1991; Sergienko, 2013), and therefore these water bodies evolve in the same location on an inter- and intra-annual basis (Banwell et al., 2014; Bell et al., 2018). By contrast, the location of surface water bodies on Antarctic ice shelves reflects variations in the surface topography, which are controlled by a combination of factors including (i) basal channels formed by ocean melting (Dow et al., 2018), (ii) basal crevassing (McGrath et al., 2012), (iii) the development of ice flow-stripes in the grounding zone (Glasser and Gudmundsson, 2012), and (iv) suture zone depressions (Bell et al., 2017). In Antarctica, these factors result in a wide range of surface water body geometries; from circular forms, to long linear features that can traverse significant distances across an ice shelf, and might therefore have significant implications for the lateral transfer of surface meltwater.

Here, we advance the work of Williamson, *et al.* (2018b) and Miles *et al.* (2017) to produce 'FASTISh', a Fully Automated Supraglacial Lake and Stream Tracking Algorithm for Ice Shelves. We develop the FASTER algorithm for use with Landsat 8 and Sentinel-2 data to make it applicable to Antarctic ice shelves. Such adaptations include: (i) assigning approximate depths to pixels with floating ice cover; (ii) acknowledging the geometric variability of surface water bodies across Antarctica and the impact this variability has on the lateral transfer of surface meltwater by categorising water bodies as either circular or linear; (iii) assigning each water body that is tracked over the melt season to one of four categories (always circular, always linear, simple transitions (from circular to linear or vice versa) and envelopment transitions (where water bodies spread and merge with neighboring circular and linear water bodies to form a new water body, or where a water body splits into smaller circular and linear water bodies) to quantify and illustrate the interaction between individual water bodies as the melt season progresses. We then apply the FASTISh

algorithm to the Nivlisen Ice Shelf, Antarctica, for the 2016-2017 melt season; the first full melt season to have data coverage over the ice shelf from both Landsat 8 and Sentinel-2.

2 Study Area

The Nivlisen Ice Shelf (70.3 °S, 11.3°E), is situated in Dronning Maud Land, East Antarctica, between the Vigrid and Lazarev ice shelves (Fig. 1). It has a surface area of 7,600 km^2, and is ~123 km wide by 92 km long. Ice thickness ranges from 150 m at the calving front to ~ 700 m towards the ice shelf's grounding line in the southeast, and it exhibits flow velocities of around 20 m a^{-1} to 130 m a^{-1} (Horwath et al., 2006). To the southeast of the Nivlisen Ice Shelf, there is a blue ice region maintained by katabatic winds, which extends in a south easterly direction for ~ 100 km (Horwath et al., 2006). This blue ice region is characterised by ablation, and adjoins the exposed bedrock nunatak (called Shirmacheroasen), which is positioned where the ice shelf meets the inland ice (Horwath et al., 2006) (Fig.1). Beyond this blue ice region, towards the north, the ice shelf transitions into an accumulation zone as the firn layer thickens (Horwath et al., 2006). In the 2016-2017 melt season, mean daily near-surface temperatures on the Nivlisen Ice Shelf ranged between ~ -25°C and 2°C, and 1.6 % of the study area occupied by a surface water body at least once during this time. The Nivlisen Ice Shelf was selected for this study as: i) pervasive surface meltwater features have previously been identified here in optical satellite imagery, showing evidence of widespread melt ponding in both circular and linear water bodies (Kingslake et al., 2017); ii) these meltwater features have shown significant development over a melt season, as source lakes upstream of the grounding line appeared to drain laterally, rapidly flooding large areas of the ice shelf (Kingslake et al., 2015); and iii) the ice shelf is relatively small, allowing quick and efficient development and application of FASTISh before its use more widely across larger Antarctic ice shelves.

3 Methods

There are four main components to the FASTISh algorithm: i) delineating water body areas; ii) calculating water body depths and volumes; iii) categorising water bodies as either circular or linear based upon their geometries; iv) tracking individual water bodies and measuring their changing dimensions and geometries over time (Fig.2). These will be discussed in sections 3.2 to 3.5 respectively, once the pre-processing steps applied to the imagery used have been outlined (section 3.1).

3.1 Images and Pre-Processing

3.1.1 Landsat 8

12 Landsat 8 scenes with minimal cloud cover, from between 1st November 2016 and 24th March 2017, and each partially covering the ice-shelf extent, were identified and downloaded from the USGS Earth Explorer website (https://earthexplorer.usgs.gov) (Fig. S1). Each scene was downloaded as a Tier 2 data product, in the form of raw digital numbers (DN). Bands 2 (blue), 3 (green), 4 (red) and 8 (panchromatic) were used for this study (Fig. 2). Bands 2, 3, and 4 have a 30 m spatial resolution, and Band 8 has a 15 m spatial

resolution. Image scene values were first converted from DN to Top-of-Atmosphere (TOA) reflectance values. Typically, Landsat scenes are converted to TOA reflectance values using a single solar angle over the whole image scene. However, here we correct each pixel for the specific solar illumination angle, based on metadata stored in the .ANG file, and using the 'Solar and View Angle Generation Algorithm' provided by NASA (https://landsat.usgs.gov/sites/default/files/documents/LSDS-1928_L8-OLI-TIRS_Solar-View-Angle-Generation_ADD.pdf). Converting from DN to TOA values on a per-pixel basis is imperative when mosaicking and comparing images obtained at high latitudes, as the solar angle at the time of acquisition can vary significantly across each scene due to the large change in longitude.

For each Landsat scene, a cloud mask was generated and downloaded from Google Earth Engine (GEE) using the 'Simple Cloud Score Algorithm' (ee.Algorithms.Landsat.simpleCloudScore). The simple cloud score algorithm assigns a 'cloud score' to every pixel in the image based on the following criteria: (i) brightness in bands 2 (blue), 3 (green), 4 (red); (ii) brightness in just band 2 (blue); (iii) brightness in bands 5 (near infrared), 6 (shortwave Infrared 1) and 7 (shortwave infrared 2); and iv) temperature in band 10 (thermal). The algorithm also uses the Normalised Difference Snow Index (NDSI) to distinguish between clouds and snow, which prevents snow from being incorrectly incorporated in the cloud mask. The NDSI was developed by Hall et al. (2001) to distinguish between snow/ice and cumulus clouds and is calculated from the following bands:

$$\text{NDSI} = (\text{Blue} - \text{Near Infrared 1})/(\text{Blue} + \text{Near Infrared 1}) \quad (1)$$

We found the 'simple cloud score algorithm' to be the most effective cloud masking method for Landsat 8 images, as it assesses each pixel using multiple criteria, making it more effective than any single band threshold. Prior to implementing the FASTISh algorithm, each Landsat scene and corresponding cloud mask was clipped to the study area extent in ArcGIS using the batch clip process. Clipping each scene to the same extent is required when comparing images through the FASTISh algorithm, as tracking individual features over time requires images with a consistent spatial reference frame to determine the location of each water body. The 12 scenes formed six pairs (Fig. S1), with two scenes per day each covering part of the ice shelf. Each scene pair was mosaicked using ArcGIS's 'mosaic to new raster' tool to produce six images providing near-complete coverage of the ice shelf for six days of the 2016-2017 melt season (Fig. S1). All images were projected into the 1984 Stereographic South Pole co-ordinate system (EPSG: 3031).

3.1.2 Sentinel-2

20 Sentinel-2A level-1C scenes obtained between 1st November 2016 and 31st March 2017 with minimal could cover were downloaded from the Copernicus Hub web site (https://scihub.copernicus.eu) (Fig. S1). Bands 2 (blue), 3 (green), 4 (red), and 11 (short wave infrared (SWIR)) were used. Bands 2, 3, and 4 have a spatial resolution of 10 m, and band 11 a spatial resolution of 20 m. The Sentinel-2 data for all bands were downloaded as

TOA reflectance values, and were divided by the 'quantification value' of 10,000 (from metadata), to convert the numbers into values that lie within the zero to one range (Traganos et al., 2018). We applied this conversion to bands 2, 3 and 4 as these are the bands used to identify water and calculate its depth, and their values need to be comparable to the values provided by Landsat 8. Each downloaded scene was clipped, mosaicked to produce images with full coverage of the ice shelf, and then re-projected to the WGS 1984 Stereographic South Pole co-ordinate system (EPSG: 3031), in line with the Landsat scenes. As the simple cloud score algorithm had not been adapted for application to S2 imagery at the time of writing, we computed a cloud mask for each image using a thresholding approach, whereby pixels were categorised as cloudy if the SWIR band value was > 10,000. This threshold was selected through visually assessing the effectiveness of various thresholds against the corresponding RGB scenes. As the resolution of the original SWIR band was 20 m, the resultant cloud masks were resampled using nearest neighbor interpolation to 10 m spatial resolution. On two image dates (14th November 2016 and 25th February 2017), this cloud masking approach was not entirely successful as not all clouds were fully masked. Additional individual masks were manually digitised in ArcGIS to ensure all clouds were masked for these images.

3.2 Delineating Water Body Areas

Water body areas were determined using the Normalised Difference Water Index for ice ($NDWI_{ice}$), which has been widely used previously to calculate the distribution of surface meltwater features on the GrIS and on Antarctic ice shelves (e.g. Yang and Smith 2013; Moussavi et al., 2016; Koziol et al. 2017; Macdonald et al. 2018; Williamson et al. 2018b; Banwell et al. 2019). It is calculated from the normalised ratio of the blue and red bands as:

$$NDWI_{ice} = (Blue - Red) / (Blue + Red) \quad (2)$$

These bands were used because water has high reflectance values in the blue band, and there is a relatively large contrast between ice and water in the red band (Yang and Smith, 2013). Studies typically apply a single $NDWI_{ice}$ threshold to an image in order to classify pixels as either 'wet' or 'dry' (e.g. Fitzpatrick et al., 2014; Moussavi et al. 2016; Miles et al. 2017). Across both Greenland and Antarctica, most studies have used a relatively high $NDWI_{ice}$ threshold of 0.25 to map 'deep' water bodies on ice (Yang and Smith 2013, Bell et al. 2017, Williamson et al. 2018b). The same approach was applied to the Nivlisen Ice Shelf in this study in order to facilitate the detection of deep water bodies only. This is important because if too much shallow water and slush is detected, identifying and subsequently tracking individual water bodies over time becomes difficult. Having applied a 0.25 $NDWI_{ice}$ threshold to each image, the resulting water masks were filtered using a two-dimensional 8-connected threshold (i.e. grouping pixels if they were connected by their edges or corners) to identify each individual water body. Water bodies consisting of ≤ 2 pixels (Landsat 8) and ≤ 18 pixels (Sentinel-2), were removed to ensure only water bodies with an area ≥ 1,800 m^2 were assessed further. To ensure that pixels with floating ice cover were still included in the analysis, we then used the 'imfill' function within MATLAB to classify any 'dry' pixels situated

within a water body as water.

3.3 Water Body Depth Calculations

Having identified the extent of water bodies, we use a physically-based approach (Sneed and Hamilton, 2007; Arnold et al., 2014; Banwell et al., 2014, 2019; Pope, 2016; Pope et al., 2016; Williamson et al., 2017, 2018b) based on the original work of Philpot (1989), to calculate pixel water depths. Water depth, *z*, is calculated from:

$$z = \frac{[\ln(A_d - R_\infty) - \ln(R_{pix} - R_\infty)]}{g} \quad (3)$$

where R_{pix} is the satellite-measured pixel reflectance, A_d is the lake-bottom albedo, R_∞ is the reflectance value for optically deep (> 40 m) water, and *g* is the coefficient associated with the losses made during downward and upwards travel in a water column.

For the Landsat 8 images, pixel water depths were calculated using TOA reflectance data for both the red and panchromatic bands separately, and then averaging these values to give a single final value (Pope *et al.*, 2016; Williamson *et al.*, 2018b). Pope et al. (2016) show that this approach gives the smallest mean difference (0.0 +/- 1.6m) between spectrally-derived and DEM-derived lake depths. However, it should be noted that owing to the rapid attenuation of red light by a water column, this algorithm is only able to retrieve depths up to a maximum of ~ 5 m (Pope et al., 2016). Furthermore, this method assumes: (i) no wind and waves at the water body surface (ii) little to no dissolved/suspended material within the water body, (iii) no inelastic scattering, and (iv) the water body substrate is parallel to the surface and homogenous (Sneed and Hamilton, 2011).

In our study, the panchromatic band was first resampled using bilinear interpolation from 15 m to 30 m spatial resolution to match the resolution of the red band. For the Sentinel-2 images, water body depths were calculated using the TOA reflectance values in the red band only, as there is no equivalent panchromatic band (Williamson *et al.* 2018b). To calculate A_d, the mean reflectance value of the second (Landsat) and sixth (Sentinel) rings of pixels outside of each water body was calculated, following a similar approach used by Arnold et al. (2014) and Banwell et al. (2014). The second or sixth ring of pixels surrounding each lake was used to avoid calculating A_d from slushy areas that border each water body; sixth-pixel rings were used for Sentinel-2 images as these represent the same distance away from the water body as two-pixel rings in Landsat images. In very rare cases, wet pixels within a water body could have a reflectance higher than the calculated A_d value, leading to negative water depths. All such pixels were removed from the area and depth matrix (Fig. 2).

Values for R_∞ were assessed on an image-by-image basis by taking the minimum reflectance value found over optically deep water (the ocean). For images that did not contain optically deep water, the R_∞ value was set to 0 (Banwell et al., 2019). For Landsat 8

imagery we used a *g* value of 0.7507 for the red band, and 0.3817 for the panchromatic band (Pope *et al.*, 2016), and for Sentinel-2 imagery, we used a value of 0.8304 (Williamson *et al.*, 2018b). Pixels that had a floating ice cover and had been filled (see section 3.2) were assigned the mean depth of their respective water bodies, as it is not possible to calculate the depth of a pixel with an ice cover. Individual water body volumes were calculated by multiplying each pixel area by its calculated water depth, and then summing across the water body. To facilitate comparisons between Landsat 8 and Sentinel-2 data, area and depth arrays generated from Landsat 8 images were then resampled to 10 m spatial resolution using nearest neighbour interpolation.

3.4 Classifying Water Body Types

Having produced area and depth masks for each date, each identified water body was categorised as either circular or linear based on its solidity (defined as the proportion of pixels of the water body that fall within its convex hull), which was calculated using the 'regionprops' function in MATLAB (Banwell et al. 2014). Linear water bodies have a solidity score closer to 0 reflecting the smaller proportion of wet pixels within the convex hull due to likely greater concavity of the edges, whereas more circular water bodies have a solidity score closer to 1 due to the larger proportion of wet pixels within the convex hull due to the more convex shape. Here, water bodies with a solidity score ≥ 0.45 were classified as circular, and water bodies with a solidity score < 0.45 were classified as linear. This threshold was selected by visually assessing the masks generated from thresholds ranging between 0.42 and 0.49, in increments of 0.01, and selecting the threshold that appears to best distinguish between more circular and more linear water bodies (Fig. 3).

3.5 Tracking Water Bodies

A 3D matrix of all water bodies was compiled, recording the area and volume of each water body over time, as well as whether the water body had a circular or linear geometry (as defined in section 3.4). To track changes in the area and volume of surface meltwater bodies throughout the 2016-2017 melt season, a maximum extent mask was also generated by superimposing the areas of all water bodies identified in each image (Williamson *et al.*, 2018b). The maximum extent mask was then used to guide the tracking process. Each individual water body within the maximum extent was prescribed an ID, and changes to the area and volume of each individual water body over time were tracked within its maximum extent (Williamson *et al.*, 2018b).

In addition to tracking changes in the area and volume of each water body, the FASTISh algorithm also tracks the water body type. From this tracking process, four categories were defined: (i) always circular, (ii) always linear, (iii) 'simple transitions' where a water body is defined as *either* circular or linear and switches between the two categories (either once or more than once, and in either direction), and (iv) 'envelopment transitions' where water bodies spread and merge with neighbouring circular and linear water bodies to form new, larger bodies, or where larger bodies split into smaller circular and linear water bodies. This

final category allows us to track the development of large surface water bodies across the ice-shelf surface as it identifies smaller water bodies being subsumed by larger water bodies as the melt season progresses.

~~3.5.1 Tracking volume loss from~~

~~Previous studies have attempted to identify rapid drainage events, defined as events where lakes lose > 80 % of their maximum volume in ≤ four days (e.g. Fitzpatrick et al., 2014; Miles et al., 2017; Williamson et al., 2018b). Here, however, the temporal resolution of available imagery for the Nivlisen Ice Shelf is not high enough to allow this. Therefore, we used the calculated volume time series to identify that lost > 80 % of their maximum volume over the full melt season, . Treferred to as 'loss events' hereafter.~~

3.6 Digital Elevation Model

To aid interpretations of the tracking results produced by the FASTISh algorithm, we used surface elevation data from the Reference Elevation Model of Antarctica (REMA) database (Howat et al., 2019). Figure 4a shows the REMA Digital Elevation Model (DEM) of the ice shelf at 8 m resolution, produced by mosaicking four, 8 m resolution REMA tiles. In addition, a single 2 m REMA data strip from 31st January 2016 was used to extract the elevation profiles along two tracked water bodies, the Eastern System and the Western System, which are introduced in section 4.2.2.

3.7 Regional climate simulation

In order to understand how climate variability influences the findings, we analysed results from an atmosphere-only regional climate CORDEX (COordinated Regional climate Downscaling Experiment) simulation of Antarctica using the limited-area configuration of Version 11.1 of the UK Met Office Unified Model (MetUM) for the period 2016-2017. The MetUM is a weather prediction model, which uses a semi-Lagrangian semi-implicit scheme for solving the fully-compressible, non-hydrostatic, deep-atmosphere equations of motion (Walters et al., 2017).

The setup of the MetUM is similar to that used by Mottram et al. (2020), with the exception that the horizontal resolution for the limited-area Antarctic domain has been increased from 50 to 12 km (and consists of 392 × 504 grid points). The Antarctic domain uses the regional atmosphere mid-latitude (RA1M) science configuration (Bush et al., 2019), a rotated latitude-longitude grid in order to ensure that the grid points are evenly spaced, and 70 vertical levels up to an altitude of 40 km.

The required start data and lateral boundary conditions for the Antarctic domain is supplied by a global version run of the MetUM at N320 resolution (640 × 480 grid points, equivalent to a horizontal resolution of 40 km at mid-latitudes), which is itself initialised by ERA-Interim atmospheric reanalysis (Dee et al., 2011). The model is used to provide a series of 12 to 24 hr forecasts, provided every 12 hrs, for the period 20151231T1200Z to 20171230T0000Z, i.e. the initial 12 hrs of each forecast is discarded as spin-up, with the remaining part of the forecasts concatenated together to form a continuous time-series for the period November 2016 to April 2017. We extracted daily mean and daily maximum near-surface diurnal air

temperatures (at a height of 1.5 m above the ground) for the model grid-point immediately to the south of Schirmacheroasen.

~~To put the calculations of meltwater volume into the context of seasonal variations in surface meltwater production rates, we used surface air temperature and ground surface temperature data for Novolazarevskaya station (70°46'04" S and 11°49'54"E), Nivlisen, downloaded from the Russian Federation NADC, Arctic and Antarctic Research Institute (AARI) (http://www.aari.aq). The station is positioned on the southeastern edge of the Shirmacheroasen, and is 80 km inland from the Lazarev Sea Coast. Monthly mean averages were plotted for the duration of the melt season (1 November 2016 - 30 April 2017).~~

4 Results

4.1 Spatial Extent and Distribution of Surface Water Bodies

The seasonal evolution of meltwater bodies during the 2016-2017 summer is shown in Figure 5. The surface meltwater system transitions from a series of small isolated water bodies clustered towards the grounding line (Fig 5A), to a connected system dominated by two linear water bodies with a length of (a) ~ 20.5 km and (b) ~ 16.9 km that propagate towards the ice-shelf front (Fig 5D).

For example, on 11th December 2016, few meltwater bodies exist, and they are predominantly clustered within the blue ice region towards the grounding line in the south-west (Fig. 5A). The majority of these water bodies exist as distinct entities, and do not connect to one another. Some meltwater ponds are identified in close proximity to the nunatak. The total volume and area of all surface meltwater bodies on the 11th December is 2.8 x 10^6 m^3 and 2.8 x 10^6 m^2 respectively (Table 1). The mean water depth is 1.0 m, and the maximum water depth is 3.4 m (Table 1). By 17th December (Fig. 5B), there has been a marked increase in the total volume (3.2 x 10^7 m^3) and area (4.7 x 10^7 m^2) of surface meltwater, held in both circular and linear surface water bodies (Table 1). The mean water depth is 0.7 m and the maximum water depth is 3.1 m (Table 1). Several of the previously isolated ponds have coalesced in some of the main topographic lows. The spatial extent of the surface water bodies extends ~ 2 km further towards the ice-shelf front. In addition, some water bodies have begun to develop towards the eastern edge of the grounding line in a blue ice region.

A marked shift in the surface meltwater system is identified by 27th December (Fig 5C), as two large linear water bodies have formed along the north-south axis (labelled a and b in Fig. 5C). The Western linear water body (a) is ~ 6.5 km long and ~ 10 km from the Eastern linear water body (b), which is ~ 8.5 km long and proximal to the surface lakes on the ice shelf's eastern margin (Fig. 5C). Overall, there are fewer isolated lakes towards the grounding line, and the majority of the surface meltwater is proximal to the two large linear systems, at elevations of ~ 60 m to 65 m (Fig. 4). The total volume and area of all surface meltwater bodies is 4.9 x 10^7 m^3 and 5.4 x 10^7 m^2 respectively (Table 1). The mean water

depth of all identified water bodies is 0.9 m and the maximum water depth is 4.7 m (Table 1).

By 26th January 2017 (Fig. 5D), the total volume and area of surface meltwater reaches a peak for the summer, at 5.5 x 10^7 m^3 and 9.1 x 10^7 m^2 respectively (Table 1). This is facilitated by the enlargement of the two large linear systems, which involves the flooding of topographic lows as water appears towards the firn further north on the ice shelf. These linear systems are now (a) ~ 20.5 km and (b) ~ 16.9 km in length, and have a mean depth of (a) 0.8 m and (b) 0.7 m. The mean depth of all water on 26th January 2017 is 0.6 m and the maximum water depth is 3.3 m (Table 1).

By 13th February (Fig 5E), the two large linear systems remain prominent on the ice shelf, but they have lost area, depth and volume at their southern ends. The mean water depth of all water is 0.6 m and the maximum water depth is 4.3 m (Table 1). The total volume and area of surface meltwater bodies falls to 3.7 x 10^7 m^3 and 6.3 x 10^7 m^2 (Table 1), reflecting the shrinkage of the two linear systems.

4.2 Tracking Results

Of the 1598 water bodies identified and tracked within the maximum extent matrix, 1458 (91%) are defined as always circular, 42 (3%) are identified as always linear, 51 (3%) are defined as simple transitions, and 47 (3%) are categorised as envelopment transitions. Water bodies that are always circular are predominantly clustered further south on the ice shelf towards the grounding line, while water bodies defined as envelopment transitions are found further north, towards the ice-shelf front (Fig. 6).

4.2.1 Total Area and Volume of Tracked Surface Water Bodies

For each of the tracked water body categories, Table 2 shows the maximum area and volume, and the corresponding dates on which these maxima were reached. The minimum area and volume for all tracked categories is zero on 14th November 2016, as no deep surface melt water was detected on that date. Although 91% of water bodies identified are classified as circular, they do not dominate the total area or volume of surface meltwater (Table 2, Fig. 7). Conversely, the envelopment transitions, of which there are only 47 in total, peak at 8.0 x 10^7 m^2 in area and 4.5 x 10^7 m^3 in volume on 26th January 2017, over a month later than the peaks in area and volume recorded for the other three categories. These envelopment transitions dominate the total area and volume signals for 'all water bodies' (Table 2), which also reach their maxima on 26th January (Table 2, Fig. 7). Between 17th December 2016 and 27th December 2016 'all water bodies' are characterised by 'deepening', as their total volume increases at a greater rate than their total area, and their mean depth increases (Tables 1 and 2, Fig. 7). Whereas between the 27th December and the 26th January, 'all water bodies' are characterised by 'spreading', as their total area increases at a faster rate than their total volume, and the mean water body depth decreases (Tables 1 and 2, Fig. 7).

4.2.2 Tracking Individual Water Bodies

In addition to quantifying total surface water area and volume for each of the four water body categories (Fig. 7, Table 2), the FASTISh algorithm also tracks changes in the area and volume of *individual* water bodies. Over the 2016-2017 melt season, the two largest envelopment transitions, referred to as the Western System (WS) and the Eastern System (ES) hereafter, propagate towards the ice-shelf front as the melt season progresses, and contain 62.6 % of the total surface water volume on 26th January 2017. The remainder of this sub-section focuses solely on presenting the tracking results for these two water bodies.

The WS is active between 11th December 2016 to 25th February 2017. The area and volume of meltwater within the WS reaches a maximum of 4.6×10^7 m^2 and 2.5×10^7 m^3 respectively on 26th January 2017 (Fig. 8). The ES has a shorter lifespan, and is active between 27th December 2016 and 25th February 2017 (Fig. 8). The area and volume of the ES peaks at 1.9×10^7 m^2 and 9.6×10^6 m^3 on the 26th January 2017. Figure 9 shows the surface elevation profiles for the WS and the ES, which are extracted from the maximum extent mask (see section 3.5). Both systems are characterised by a surface sloping downwards towards the ice-shelf front. The WS has a very shallow slope, with the elevation decreasing by ~ 2 m over the 25.7 km profile (Fig. 9a); the ES is slightly steeper, showing a ~ 6 m decrease in elevation over its 27 km profile (Fig. 9b).

4.2.3 Identifying Individual Lake Freeze Through/Drainage Events.

Previous studies have attempted to identify rapid drainage events, defined as events where lakes lose > 80 % of their maximum volume in ≤ four days (e.g. Fitzpatrick et al., 2014; Miles et al., 2017; Williamson et al., 2018b). Here, however, the temporal resolution of available imagery for the Nivlisen Ice Shelf is not high enough to allow this. Therefore, we used the calculated volume time series to identify water bodies in the 'always circular' category that lost > 80 % of their maximum volume over the full melt season, through either drainage or freeze through. We focus solely on the 'always circular' category to better understand the local loss of surface melt water in seemingly isolated and stationary water bodies. These events are referred to as 'loss events' hereafter.

Figure 10 shows the loss in water volume through freeze-through or drainage for the 'always circular' category over the melt season, together with the seven day moving average for the mean daily and daily maximum near-surface air temperatures over the ice shelf from the MetUM simulation. This shows that 805 lakes have a 'loss event' by 18th December 2017, losing a total volume of 1.5×10^7 m^3, which occurs following sustained relatively warmer atmospheric conditions since the beginning of December 2016, e.g. characterised by daily maximum near-surface air temperatures reaching 0°C.

5 Discussion

5.1 Spatial and Temporal Distribution of Surface Meltwater Bodies

In the early melt season, surface meltwater on the Nivlisen Ice Shelf ponds in small surface lakes that form in relatively flat areas towards the grounding line, in close proximity to Shirmacheroasen and the blue ice regions (Figs. 4 and 5). This initial generation of surface meltwater is likely driven by regional wind patterns and the effects of local ice-albedo, as the relatively low albedo of the blue ice can lead to increased local melt rates (Lenaerts et al., 2017; Bell et al., 2018; Stokes et al., 2019). Furthermore, areas of lower elevation towards the grounding line are likely to be exposed to katabatic winds, which can result in near-surface temperatures that are 3 K greater than temperatures further up-ice and down-ice (Lenaerts et al. 2017). These persistent katabatic winds can also result in the production of blue ice regions, as snow is eroded from the ice-shelf surface (Lenaerts et al., 2017). Our results for the early melt season on the Nivlisen Ice Shelf therefore support the findings of Kingslake et al. (2017) who found, for a variety of ice shelves around Antarctica, that 50 % of the ice-shelf drainage systems are either within 8 km of rock exposures, or within 3.6 km of blue ice surfaces.

Seasonal variations in the amount of surface meltwater on the Nivlisen Ice Shelf are driven by temperature fluctuations, with increases in surface water area and volume corresponding with rising mean daily near-surface temperatures and daily maximum near-surface temperatures (Fig. 10). However, as the melt season progresses, there is a transition to a connected surface drainage network, which facilitates a progressive transfer of surface meltwater away from the grounding line towards the ice-shelf front. As mean daily and daily maximum temperatures rise and surface water bodies increase in area and volume (Fig.10), they grow, merge with nearby water bodies, and form new extended networks of surface water on the ice-shelf surface. While rising near-surface temperatures are a strong control on the amount of surface meltwater, the direction and extent of the identified lateral water transfer is controlled by the ice shelf's surface topography (Fig. 4b). Over the course of the melt season, the area and volume of surface meltwater decreases in the regions close to the grounding line, and increases in more distal parts of the ice shelf.

The development of the two largest enveloping water bodies (WS and ES) dominate the transition to a generally more connected drainage network. This is because these systems facilitate large-scale transfer of water across the shelf, as water ponds within linear depressions. The ES and WS appear to be fed by smaller circular and linear surface meltwater bodies, and as the area and volume of the ES and WS increases, they spread and envelope nearby water bodies. Smaller water bodies likely contribute surface melt to the ES and WS by (i) overtopping their local basin sides and flowing over impermeable ice, which may be refrozen surface or shallow subsurface meltwater from previous years (Kingslake et al., 2015) or (ii) percolating into the firn pack and spreading laterally towards the ES and WS. However, the 'pulse' forward of the ES and WS between 27th December 2016 and 26th January 2017 does not appear to be controlled by a topographic 'lip' or 'dam'. It is therefore likely to primarily be the result of increased meltwater production, resulting in saturation of the surrounding firn pack, which may bring it up to isothermal conditions, thereby facilitating further melt and lateral transfer.

By 26th January 2017, the ES and WS are the dominant features within the entire Nivlisen Ice Shelf meltwater system, together holding 62.6% of the surface meltwater volume. On this date, the ES and WS reach a length of ~ 16.9 km and ~ 20.5 km respectively, although unlike observations on the Nansen Ice Shelf (Bell et al., 2017), they do not facilitate the export of surface meltwater off the ice-shelf front via a waterfall. Instead, both systems always terminate at least ~ 35 – 55 km from the ice-shelf front, suggesting that the water percolates into the surrounding firn in that area of the ice shelf. This interpretation is supported by Figure 11 which shows a Sentinel-1 SAR image (Fig 11b), from 26th January 2017 together with the Sentinel-2 image (Fig 11a). Areas of low backscatter (appearing as dark areas in the image) are widespread across the tributary glaciers and extend across the grounding line onto the upper part of the ice shelf. Whilst areas of low backscatter may result from snow-grain size, surface topography/roughness, and internal stratigraphy (Rott and Mätzler, 1987), it seems more likely that areas of low backscatter north of the blue ice areas represent saturated firn and/or surface melt (Bindschadler and Vornberger, 1992; Miles et al., 2017). Areas of low backscatter clearly extend beyond areas of visible surface melt in the optical imagery, indicating the presence of subsurface meltwater. For example, there are prominent areas of low backscatter (~ - 5 to -15 dB) extending ~ 10 km north of both the ES and WS as detected by FASTISh (Fig 11b). This shows that the linear water features visible in the optical imagery are part of much larger water bodies, with a lot of the water existing as slush at the surface or in the shallow subsurface.

Whilst the drainage system currently observed on the Nivlisen Ice Shelf does not transfer surface meltwater all the way to the ice-shelf front, it is plausible that such a system could develop in the future as the quantity of surface meltwater produced increases. Whilst the water may pond, (possibly resulting in eventual hydrofracture and ice-shelf collapse), the ES and WS may also evolve quickly and efficiently, over increasingly saturated firn layers, to allow water to flow off the ice-shelf front, thereby exporting some excess meltwater and mitigating the potential threat to the ice shelf (Bell et al., 2017; Banwell, 2017).

Overall, 1.6 % of the Nivlisen Ice Shelf is occupied by some form of surface meltwater body at some point during the 2016-2017 melt season, and over those areas, the mean water depth is 0.85 m. Comparatively, prior to its collapse, 5.3 % the Larsen B Ice Shelf was covered by a surface meltwater body, and the mean water depth was 0.82 m (Banwell et al., 2014). Whilst the mean water body depths between the Larsen B and Nivlisen Ice Shelves are comparable, the spatial distributions of these water bodies, and the proportion of the ice shelf that they cover, are different. Surface water bodies were distributed relatively evenly across the entire surface of Larsen B before it collapsed, whereas surface water bodies are predominantly clustered towards the grounding line on the Nivlisen Ice Shelf, and the transfer of surface melt towards the ice-shelf front and across snow/firn-covered regions is predominantly facilitated by the larger WS and ES. The development of these large, linear water bodies is likely facilitated by topography, and allows the transfer of summer meltwater towards the ice-shelf front. This large scale lateral transfer of meltwater is further facilitated

as the ES and WS develop over frozen meltwater paths from previous years (Kingslake et al., 2015). ~~The relatively extensive snow and firn cover on the Nivlisen Ice Shelf likely prevents the development of a similar meltwater distribution to that observed on the Larsen B Ice Shelf, as much of the surface meltwater is able to percolate into available pore space.~~

5.2 Loss of Water Volume from Circular Surface Water Bodies

The loss of 1.5 x 10^7 m^3 of surface water from the circular water bodies by 27th December 2017 follows sustained relatively warmer atmospheric conditions since the beginning of December 2017 (Fig. 10), and coincides with an increase in the total surface water volume on the ice shelf (Fig 10b). In particular, we see an increase in the volume of water held within the enveloping water bodies, which continues to increase up to a maximum of 4.5 x 10^7 m^3 on 26th January 2017 (Fig. 7). It is likely, therefore, that the loss of water from circular water bodies at this early stage in the melt season signifies the lateral transfer of water away from the small 'isolated' bodies near the grounding line into the large enveloping water bodies which hold and transport the surface meltwater across the ice shelf to more distal regions. This lateral transfer of water may be occurring through two mechanisms: (i) the over-topping of surface lakes, which results in the formation of shallow channels that connect water bodies and facilitate the transfer of water towards the ice-shelf front (e.g. Banwell et al., 2019), or (ii) the gradual percolation of surface meltwater into the cold firn pack, which reduces the firn air content (FAC) of a region (Lenaerts et al., 2017), therefore creating an impermeable surface over which water can flow (e.g. Kingslake et al., 2015). The firn may also become saturated enough to be isothermal, therefore melting and facilitating the flow of upstream ponded meltwater. This is particularly likely to occur near surface depressions such as those that are later occupied by the WS and ES.

5.3 Potential Implications for Ice-Shelf Stability

It is expected that the area of coverage and volume of surface meltwater on Antarctic ice shelves will increase into the future, in line with rising atmospheric temperatures (Bell et al., 2018; IPCC, 2019; Kingslake et al., 2017; Siegert et al., 2019). This surface water may have significant implications for ice-shelf stability, as meltwater accumulation can lead to hydrofracture which could subsequently result in the collapse of an ice shelf, as seen on the Larsen B Ice Shelf in 2002 (Robel and Banwell, 2019; Banwell et al., 2013). An ice shelf may become increasingly vulnerable to hydrofracture if its FAC is reduced (Lenaerts et al., 2017). On ice shelves like Nivlisen, where large-scale lateral water transfer prevails, meltwater is delivered to locations that may otherwise not receive or experience much melt (Bell et al., 2017), and the FAC of these locations will, in turn, be reduced, increasing their susceptibility to surface meltwater ponding and hydrofracture.

Surface meltwater re-freezing at the end of the melt season will also act as a significant source of heat, and the lateral transfer of surface melt could cause increased warming of the ice shelf and possible weakening in areas which currently do not experience significant

summer melt. Were the maximum volume of surface meltwater we observe on the Nivlisen Ice Shelf in the 2016-2017 melt season (5.5 x 10^7 m^3) to re-freeze over the maximum area of surface meltwater (9.1 x 10^7 m^2), it would release an amount of energy equivalent to 49 days of potential solar energy receipts (calculated using the methods of Arnold and Rees (2009)), assuming an ice surface albedo of 0.86; the mean value calculated for a water-free distal area of the ice shelf. Furthermore, large-scale lateral water transfer and subsequent ponding may lead to ice-shelf flexure (and therefore potential fracture) at locations that may have otherwise not been affected by flexure in response to meltwater loading (Banwell et al., 2013, 2019; Macayeal and Sergienko, 2013). However, evidence of lateral water transfer and export off the Nansen Ice Shelf has highlighted the potential for surface drainage systems to mitigate some of these meltwater driven instabilities (Bell et al., 2017).

6 Conclusions

We have adapted the pre-existing FASTER algorithm, developed for studying lakes on the GrIS (Williamson et al., 2018b), so that we can identify and track the area, depth and volume of water bodies across Antarctic ice shelves. We refer to this new algorithm as FASTISh, and have used it to study the changing geometry and spatial patterns of water bodies across the Nivlisen Ice Shelf in the 2016-2017 melt season. In total, we identify and track 1598 water bodies on the ice shelf over the course of the melt season. Surface water is initially generated towards the nunatak and blue ice region, in proximity to the grounding line. This region is relatively flat and has a low albedo, and we therefore observe localised ponding of surface meltwater. As the melt season progresses and mean daily and daily maximum temperatures increase, we see a transition from isolated, localised ponding towards the grounding line to a more connected drainage system that is influenced by the ice-shelf topography. The middle of the melt season (e.g. 27th December 2016) is characterised by the progression of surface melt water bodies towards the ice-shelf front, as two large extensive drainage systems (the East System (ES) and West System (WS)) develop in long linear surface depressions. Around the peak of the melt season (26th January 2017), the ES and WS have developed to their largest observed extent, and facilitate the lateral transfer of surface melt up to 16.9 and 20.5 km north, into the firn pack and towards the ice-shelf front. The transfer of surface meltwater to regions on the ice shelf that otherwise experience little surface melt may have implications for the structure and stability of the ice shelf in the future. Our findings could be useful in comparing to IceSat 2 derived lake depths, in addition to constraining future ice-shelf surface hydrology models.

Code and Data Availability

The satellite imagery, REMA data, and meteorological data are all open access (see section 3). The MATLAB scripts used to process the data will be freely available from Apollo Repository (https://www.repository.cam.ac.uk/) upon publication.

Author Contributions

RLD developed the methodology and scripts, building on the prior work of AGW. NSA developed the script to convert Landsat DN values to per-pixel TOA values. AO performed the Regional Climate Model run using the Met Office Unified Model to provide the meteorological data. RLD conducted all other analysis and wrote the draft manuscript, under the supervision of all other authors. All authors discussed the results and were involved in editing of the manuscript.

Competing Interests

The authors declare no competing interests

Acknowledgements

We sincerely thank Mahsa Moussavi and Allen Pope for their guidance and many productive discussions over the past two years. Rebecca Dell acknowledges support from a Natural Environment Research Council Doctoral Training Partnership Studentship (Grant number: NE/L002507/1; CASE Studentship with the British Antarctic Survey). Ian Willis acknowledges support from NERC Grant G102130. This paper was written while Ian Willis was in receipt of a Cooperative Institute for Research in Environmental Science (CIRES) Visiting Sabbatical Fellowship and he thanks in particular Waleed Abdalati, Ted Scambos, Kristy Tiampo and Mike Willis for their hospitality. Alison Banwell acknowledges support from a CIRES Visiting Postdoctoral Fellowship and a grant from the US National Science Foundation (#1841607) awarded to the University of Colorado, Boulder. AO thanks Tony Phillips (BAS) for converting the MetUM output to daily averaged fields. DEMs provided by the Byrd Polar and Climate Research Center and the Polar Geospatial Center under NSF-OPP awards 1543501, 1810976, 1542736, 1559691, 1043681, 1541332, 0753663, 1548562, 1238993 and NASA award NNX10AN61G. Computer time provided through a Blue Waters Innovation Initiative. DEMs produced using data from DigitalGlobe, Inc.

References

Arnold, N. and Rees, G.: Effects of digital elevation model spatial resolution on distributed calculations of solar radiation loading on a high arctic glacier, J. Glaciol., 55(194), 973–984, doi:10.3189/002214309790794959, 2009.

Arnold, N. S., Banwell, A. F. and Willis, I. C.: High-resolution modelling of the seasonal evolution of surface water storage on the Greenland Ice Sheet, Cryosph., 8(4), 1149–1160, doi:10.5194/tc-8-1149-2014, 2014.

Banwell, A.: Glaciology: Ice-shelf stability questioned, Nature, 544(7650), 306–307, doi:10.1038/544306a, 2017.

Banwell, A. F. and MacAyeal, D. R.: Ice-shelf fracture due to viscoelastic flexure stress induced by fill/drain cycles of supraglacial lakes, Antarct. Sci., 27(6), 587–597, doi:10.1017/S0954102015000292, 2015.

Banwell, A. F., MacAyeal, D. R. and Sergienko, O. V.: Breakup of the Larsen B Ice Shelf

752 triggered by chain reaction drainage of supraglacial lakes, Geophys. Res. Lett., 40(22),
753 5872–5876, doi:10.1002/2013GL057694, 2013.
754 Banwell, A. F., Caballero, M., Arnold, N. S., Glasser, N. F., Cathles, L. Mac and MacAyeal,
755 D. R.: Supraglacial lakes on the Larsen B ice shelf, Antarctica, and at Paakitsoq, West
756 Greenland: A comparative study, Ann. Glaciol., 55(66), 1–8,
757 doi:10.3189/2014AoG66A049, 2014.
758 Banwell, A. F., Willis, I. C., Macdonald, G. J., Goodsell, B. and MacAyeal, D. R.: Direct
759 measurements of ice-shelf flexure caused by surface meltwater ponding and drainage,
760 Nat. Commun., 10(1), 1–10, doi:10.1038/s41467-019-08522-5, 2019.
761 Bell, R. E., Chu, W., Kingslake, J., Das, I., Tedesco, M., Tinto, K. J., Zappa, C. J.,
762 Frezzotti, M., Boghosian, A. and Lee, W. S.: Antarctic ice shelf potentially stabilized by
763 export of meltwater in surface river, Nature, 544(7650), 344–348,
764 doi:10.1038/nature22048, 2017.
765 Bell, R. E., Banwell, A. F., Trusel, L. D. and Kingslake, J.: Antarctic surface hydrology and
766 impacts on ice-sheet mass balance, Nat. Clim. Chang., 8(12), 1044–1052,
767 doi:10.1038/s41558-018-0326-3, 2018.
768 Bevan, S. L., Luckman, A., Hubbard, B., Kulessa, B., Ashmore, D., Kuipers Munneke, P.,
769 O'Leary, M., Booth, A., Sevestre, H. and McGrath, D.: Centuries of intense surface melt on
770 Larsen C Ice Shelf, Cryosphere, 11(6), 2743–2753, doi:10.5194/tc-11-2743-2017, 2017.
771 Bindschadler, R. and Vornberger, P.: Interpretation of SAR imagery of the Greenland ice
772 sheet using coregistered TM imagery, Remote Sens. Environ., 42(3), 167–175 [online]
773 Available from: https://www.sciencedirect.com/science/article/pii/003442579290100X
774 (Accessed 15 May 2018), 1992.
775 Bush, M., Allen, T., Bain, C., Boutle, I., Edwards, J., Finnenkoetter, A., Franklin, C.,
776 Hanley, K., Lean, H., Lock, A., Manners, J., Mittermaier, M., Morcrette, C., North, R.,
777 Petch, J., Short, C., Vosper, S., Walters, D., Webster, S., Weeks, M., Wilkinson, J., Wood,
778 N. and Zerroukat, M.: The first Met Office Unified Model/JULES Regional Atmosphere and
779 Land configuration, RAL1, Geosci. Model Dev. Discuss., 1–47, doi:10.5194/gmd-2019-
780 130, 2019.
781 Cook, A. J. and Vaughan, D. G.: Overviewing of areal changes of the ice shelves on the
782 Antarctic Peninsula over the past 50 years, Cryosph., 4, 77–98 [online] Available from:
783 http://dro.dur.ac.uk/20037/1/20037.pdf (Accessed 7 June 2018), 2010.
784 Datta, R. T., Tedesco, M., Fettweis, X., Agosta, C., Lhermitte, S., Lenaerts, J. T. M. and
785 Wever, N.: The Effect of Foehn-Induced Surface Melt on Firn Evolution Over the Northeast
786 Antarctic Peninsula, Geophys. Res. Lett., 46(7), 3822–3831, doi:10.1029/2018GL080845,
787 2019.
788 DeConto, R. M. and Pollard, D.: Contribution of Antarctica to past and future sea-level rise,
789 Nature, 531(7596), 591–597, doi:10.1038/nature17145, 2016.
790 Dee, D. P., Uppala, S. M., Simmons, A. J., Berrisford, P., Poli, P., Kobayashi, S., Andrae,
791 U., Balmaseda, M. A., Balsamo, G., Bauer, P., Bechtold, P., Beljaars, A. C. M., van de
792 Berg, L., Bidlot, J., Bormann, N., Delsol, C., Dragani, R., Fuentes, M., Geer, A. J.,
793 Haimberger, L., Healy, S. B., Hersbach, H., Hólm, E. V., Isaksen, L., Kållberg, P., Köhler,
794 M., Matricardi, M., Mcnally, A. P., Monge-Sanz, B. M., Morcrette, J. J., Park, B. K.,
795 Peubey, C., de Rosnay, P., Tavolato, C., Thépaut, J. N. and Vitart, F.: The ERA-Interim
796 reanalysis: Configuration and performance of the data assimilation system, Q. J. R.
797 Meteorol. Soc., 137(656), 553–597, doi:10.1002/qj.828, 2011.
798 Dow, C. F., Lee, W. S., Greenbaum, J. S., Greene, C. A., Blankenship, D. D., Poinar, K.,
799 Forrest, A. L., Young, D. A. and Zappa, C. J.: Basal channels drive active surface
800 hydrology and transverse ice shelf fracture, Sci. Adv., 4(6), eaao7212,
801 doi:10.1126/sciadv.aao7212, 2018.

802 Echelmeyer, K., Clarke, T. S. and Harrison, W. D.: Surficial glaciology of Jakobshavns
803 Isbrae, West Greenland: part I. Surface morphology, J. Glaciol., 37(127), 368–382,
804 doi:10.1017/S0022143000005803, 1991.
805 Fitzpatrick, A. A. W., Hubbard, A. L., Box, J. E., Quincey, D. J., Van As, D., Mikkelsen, A.
806 P. B., Doyle, S. H., Dow, C. F., Hasholt, B. and Jones, G. A.: A decade (2002-2012) of
807 supraglacial lake volume estimates across Russell Glacier, West Greenland, Cryosphere,
808 8(1), 107–121, doi:10.5194/tc-8-107-2014, 2014.
809 Fürst, J. J., Durand, G., Gillet-Chaulet, F., Tavard, L., Rankl, M., Braun, M. and
810 Gagliardini, O.: The safety band of Antarctic ice shelves, Nat. Clim. Chang., 6(5), 479–482,
811 doi:10.1038/nclimate2912, 2016.
812 Glasser, N. F. and Gudmundsson, G. H.: Longitudinal surface structures (flowstripes) on
813 Antarctic glaciers, Cryosphere, 6(2), 383–391, doi:10.5194/tc-6-383-2012, 2012.
814 Glasser, N. F. and Scambos, T. A.: A structural glaciological analysis of the 2002 Larsen B
815 ice-shelf collapse, J. Glaciol., 54(184), 3–16, doi:10.3189/002214308784409017, 2008.
816 Gudmundsson, G. H., Paolo, F. S., Adusumilli, S. and Fricker, H. A.: Instantaneous
817 Antarctic ice-sheet mass loss driven by thinning ice shelves, Geophys. Res. Lett.,
818 2019GL085027, doi:10.1029/2019GL085027, 2019.
819 Hall, D. K., Branch, H. S., Tait, A. B., Riggs, G. A., Corporation, D. S., Salomonson, V. V,
820 Directorate, E. S., Chien, J. Y. L., Corporation, G. S. and Klein, A. G.: Algorithm
821 Theoretical Basis Document (ATBD) for the MODIS Snow-, Lake Ice- and Sea Ice-
822 Mapping Algorithms, Analysis [online] Available from:
823 https://eospso.gsfc.nasa.gov/sites/default/files/atbd/atbd_mod10.pdf (Accessed 21 April
824 2019), 2001.
825 Horwath, M., Dietrich, R., Baessler, M., Nixdorf, U., Steinhage, D., Fritzsche, D., Damm, V.
826 and Reitmayr, G.: Nivlisen, an Antarctic ice shelf in Dronning Maud Land: Geodetic-
827 glaciological results from a combined analysis of ice thickness, ice surface height and ice-
828 flow observations, J. Glaciol., 52(176), 17–30, doi:10.3189/172756506781828953, 2006.
829 Howat, I. M., Porter, C., Smith, B. E., Noh, M. J. and Morin, P.: The reference elevation
830 model of antarctica, Cryosphere, 13(2), 665–674, doi:10.5194/tc-13-665-2019, 2019.
831 Hubbard, B., Luckman, A., Ashmore, D. W., Bevan, S., Kulessa, B., Kuipers Munneke, P.,
832 Philippe, M., Jansen, D., Booth, A., Sevestre, H., Tison, J. L., O'Leary, M. and Rutt, I.:
833 Massive subsurface ice formed by refreezing of ice-shelf melt ponds, Nat. Commun., 7,
834 doi:10.1038/ncomms11897, 2016.
835 Hui, F., Ci, T., Cheng, X., Scambos, T. A., Liu, Y., Zhang, Y., Chi, Z., Huang, H., Wang, X.,
836 Wang, F., Zhao, C., Jin, Z. and Wang, K.: Mapping blue-ice areas in Antarctica using
837 ETM+ and MODIS data, Ann. Glaciol., 55(66), 129–137, doi:10.3189/2014AoG66A069,
838 2014.
839 IPCC: Special Report on the Ocean and Cryosphere in a Changing Climate - Technical
840 Summary (Final Draft). [online] Available from: https://www.ipcc.ch/srocc/ (Accessed 18
841 December 2019), 2019.
842 Kingslake, J., Ng, F. and Sole, A.: Modelling channelized surface drainage of supraglacial
843 lakes, J. Glaciol., 61(225), 185–199, doi:10.3189/2015JoG14J158, 2015.
844 Kingslake, J., Ely, J. C., Das, I. and Bell, R. E.: Widespread movement of meltwater onto
845 and across Antarctic ice shelves, Nature, 544(7650), 349–352, doi:10.1038/nature22049,
846 2017.
847 Koziol, C., Arnold, N., Pope, A. and Colgan, W.: Quantifying supraglacial meltwater
848 pathways in the Paakitsoq region, West Greenland, J. Glaciol., 63(239), 464–476,
849 doi:10.1017/jog.2017.5, 2017.
850 Kuipers Munneke, P., Ligtenberg, S. R. M., Van Den Broeke, M. R. and Vaughan, D. G.:
851 Firn air depletion as a precursor of Antarctic ice-shelf collapse, J. Glaciol., 60(220), 205–

852 214, doi:10.3189/2014JoG13J183, 2014.
853 Langley, E. S., Leeson, A. A., Stokes, C. R. and Jamieson, S. S. R.: Seasonal evolution of
854 supraglacial lakes on an East Antarctic outlet glacier, Geophys. Res. Lett., 43(16), 8563–
855 8571, doi:10.1002/2016GL069511, 2016.
856 Leeson, A. A., Forster, E., Rice, A., Gourmelen, N. and van Wessem, J. M.: Evolution of
857 Supraglacial Lakes on the Larsen B Ice Shelf in the Decades Before it Collapsed,
858 Geophys. Res. Lett., 47(4), doi:10.1029/2019GL085591, 2020.
859 Lenaerts, J., Lhermitte, S., Drews, R., Ligtenberg, S. R. M., Berger, S., Helm, V., Smeets,
860 P. C. J. P., van den Broeke, M. R., van De Berg, W. J., van Meijgaard, E., Eijkelboom, M.,
861 Eisen, O. and Pattyn, F.: Meltwater produced by wind – albedo interaction stored in an
862 East Antarctic ice shelf, Nat. Clim. Chang., 7, 58–63, doi:10.1038/NCLIMATE3180, 2017.
863 Liston, G. E. and Winther, J. G.: Antarctic surface and subsurface snow and ice melt
864 fluxes, J. Clim., 18(10), 1469–1481, doi:10.1175/JCLI3344.1, 2005.
865 Liston, G. E., Winther, J. G., Bruland, O., Elvehøy, H. and Sand, K.: Below-surface ice
866 melt on the coastal Antarctic ice sheet, J. Glaciol., 45(150), 273–285,
867 doi:10.3189/s0022143000001775, 1999.
868 Luckman, A., Elvidge, A., Jansen, D., Kulessa, B., Kuipers Munneke, P., King, J. and
869 Barrand, N. E.: Surface melt and ponding on Larsen C Ice Shelf and the impact of föhn
870 winds, Antarct. Sci., 26(6), 625–635, doi:10.1017/S0954102014000339, 2014.
871 Macayeal, D. R. and Sergienko, O. V.: The flexural dynamics of melting ice shelves, Ann.
872 Glaciol., 54(63), 1–10, doi:10.3189/2013AoG63A256, 2013.
873 Macdonald, G. J., Banwell, A. F. and Macayeal, D. R.: Seasonal evolution of supraglacial
874 lakes on a floating ice tongue , Petermann Glacier , Greenland, , 1–10,
875 doi:10.1017/aog.2018.9, 2018.
876 McGrath, D., Steffen, K., Rajaram, H., Scambos, T., Abdalati, W. and Rignot, E.: Basal
877 crevasses on the Larsen C Ice Shelf, Antarctica: Implications for meltwater ponding and
878 hydrofracture, Geophys. Res. Lett., 39(16), n/a-n/a, doi:10.1029/2012GL052413, 2012.
879 Miles, K. E., Willis, I. C., Benedek, C. L., Williamson, A. G. and Tedesco, M.: Toward
880 Monitoring Surface and Subsurface Lakes on the Greenland Ice Sheet Using Sentinel-1
881 SAR and Landsat-8 OLI Imagery, Front. Earth Sci., 5, doi:10.3389/feart.2017.00058, 2017.
882 Mottram, R., Hansen, N., Kittel, C., Wessem, M. van, Agosta, C., Amory, C., Boberg, F.,
883 Berg, W. J. van de, Fettweis, X., Gossart, A., Meijgaard, E. van, Orr, A., Phillips, T.,
884 Webster, S., Simonsen, S. and Souverijns, N.: What is the Surface Mass Balance of
885 Antarctica? An Intercomparison of Regional Climate Model Estimates, Cryosph. Discuss.,
886 1–42, doi:10.5194/tc-2019-333, 2020.
887 Mouginot, J., Scheuchl, B. and Rignot., E.: MEaSUREs Antarctic Boundaries for IPY 2007-
888 2009 from Satellite Radar, Version 2., NASA Natl. Snow Ice Data Cent. Distrib. Act. Arch.
889 Center., doi:https://doi.org/10.5067/AXE4121732AD, 2017.
890 Moussavi, M. S., Abdalati, W., Pope, A., Scambos, T., Tedesco, M., MacFerrin, M. and
891 Grigsby, S.: Derivation and validation of supraglacial lake volumes on the Greenland Ice
892 Sheet from high-resolution satellite imagery, Remote Sens. Environ., 183, 294–303,
893 doi:10.1016/j.rse.2016.05.024, 2016.
894 Philpot, W. D.: Bathymetric mapping with passive multispectral imagery, Appl. Opt., 28(8),
895 1569, doi:10.1364/ao.28.001569, 1989.
896 Pope, A.: Reproducibly estimating and evaluating supraglacial lake depth with Landsat 8
897 and other multispectral sensors, Earth Sp. Sci., 3(4), 176–188,
898 doi:10.1002/2015EA000125, 2016.
899 Pope, A., Scambos, T. A., Moussavi, M., Tedesco, M., Willis, M., Shean, D. and Grigsby,
900 S.: Estimating supraglacial lake depth in West Greenland using Landsat 8 and comparison
901 with other multispectral methods, Cryosphere, 10(1), 15–27, doi:10.5194/tc-10-15-2016,

2016.
Rignot, E., Casassa, G., Gogineni, P., Krabill, W., Rivera, A. and Thomas, R.: Accelerated ice discharge from the Antarctic Peninsula following the collapse of Larsen B ice shelf, Geophys. Res. Lett., 31(18), L18401, doi:10.1029/2004GL020697, 2004.
Rignot, E., Mouginot, J., Scheuchl, B., Van Den Broeke, M., Van Wessem, M. J. and Morlighem, M.: Four decades of Antarctic ice sheet mass balance from 1979–2017, Proc. Natl. Acad. Sci. U. S. A., 116(4), 1095–1103, doi:10.1073/pnas.1812883116, 2019.
Robel, A. A. and Banwell, A. F.: A Speed Limit on Ice Shelf Collapse Through Hydrofracture, Geophys. Res. Lett., 46(21), 12092–12100, doi:10.1029/2019GL084397, 2019.
Rott, H. and Mätzler, C.: Possibilities and Limits of Synthetic Aperture Radar for Snow and Glacier Surveying, Ann. Glaciol., 9, 195–199, doi:10.3189/s0260305500000604, 1987.
De Rydt, J., Gudmundsson, G. H., Rott, H. and Bamber, J. L.: Modeling the instantaneous response of glaciers after the collapse of the Larsen B Ice Shelf, Geophys. Res. Lett., 42(13), 5355–5363, doi:10.1002/2015GL064355, 2015.
Scambos, T., Hulbe, C. and Fahnestock, M.: Climate-induced ice shelf disintegration in the Antrctic Peninsula, in Antarctica Peninsula climate variability: a historical and paleo-environmental perspective, pp. 79–92., 2003.
Scambos, T., Fricker, H. A., Liu, C. C., Bohlander, J., Fastook, J., Sargent, A., Massom, R. and Wu, A. M.: Ice shelf disintegration by plate bending and hydro-fracture—Satellite observations and model results of the 2008 Wilkins ice shelf break-ups, Earth Planet. Sci. Lett., 280ID–6, 51–60, doi:10.1016/j.epsl.2008.12.027, 2009.
Scambos, T. A., Bohlander, J. A., Shuman, C. A. and Skvarca, P.: Glacier acceleration and thinning after ice shelf collapse in the Larsen B embayment, Antarctica, Geophys. Res. Lett., 31(18), L18402, doi:10.1029/2004GL020670, 2004.
Selmes, N., Murray, T. and James, T. D.: Fast draining lakes on the Greenland Ice Sheet, Geophys. Res. Lett., 38(15), n/a-n/a, doi:10.1029/2011GL047872, 2011.
Selmes, N., Murray, T. and James, T. D.: Characterizing supraglacial lake drainage and freezing on the Greenland Ice Sheet, Cryosph. Discuss., 7(1), 475–505, doi:10.5194/tcd-7-475-2013, 2013.
Sergienko, O. V.: Glaciological twins: Basally controlled subglacial and supraglacial lakes, J. Glaciol., 59(213), 3–8, doi:10.3189/2013JoG12J040, 2013.
Siegert, M., Atkinson, A., Banwell, A., Brandon, M., Convey, P., Davies, B., Downie, R., Edwards, T., Hubbard, B., Marshall, G., Rogelj, J., Rumble, J., Stroeve, J. and Vaughan, D.: The Antarctic Peninsula under a 1.5°C global warming scenario, Front. Environ. Sci., 7(JUN), doi:10.3389/fenvs.2019.00102, 2019.
Sneed, W. A. and Hamilton, G. S.: Evolution of melt pond volume on the surface of the Greenland Ice Sheet, Geophys. Res. Lett., 34(3), L03501, doi:10.1029/2006GL028697, 2007.
Sneed, W. A. and Hamilton, G. S.: Validation of a method for determining the depth of glacial melt ponds using satellite imagery, Ann. Glaciol., 52(59), 15–22, doi:10.3189/172756411799096240, 2011.
Stokes, C. R., Sanderson, J. E., Miles, B. W. J., Jamieson, S. S. R. and Leeson, A. A.: Widespread distribution of supraglacial lakes around the margin of the East Antarctic Ice Sheet, Sci. Rep., 9(1), doi:10.1038/s41598-019-50343-5, 2019.
Traganos, D., Poursanidis, D., Aggarwal, B., Chrysoulakis, N. and Reinartz, P.: Estimating satellite-derived bathymetry (SDB) with the Google Earth Engine and sentinel-2, Remote Sens., 10(6), 859, doi:10.3390/rs10060859, 2018.
Vieli, A., Payne, A. J., Du, Z. and Shepherd, A.: Numerical modelling and data assimilation of the Larsen B ice shelf, Antarctic Peninsula, Philos. Trans. R. Soc. A Math. Phys. Eng.

Sci., 364(1844), 1815–1839, doi:10.1098/rsta.2006.1800, 2006.
Walters, D., Boutle, I., Brooks, M., Melvin, T., Stratton, R., Vosper, S., Wells, H., Williams, K., Wood, N., Allen, T., Bushell, A., Copsey, D., Earnshaw, P., Edwards, J., Gross, M., Hardiman, S., Harris, C., Heming, J., Klingaman, N., Levine, R., Manners, J., Martin, G., Milton, S., Mittermaier, M., Morcrette, C., Riddick, T., Roberts, M., Sanchez, C., Selwood, P., Stirling, A., Smith, C., Suri, D., Tennant, W., Luigi Vidale, P., Wilkinson, J., Willett, M., Woolnough, S. and Xavier, P.: The Met Office Unified Model Global Atmosphere 6.0/6.1 and JULES Global Land 6.0/6.1 configurations, Geosci. Model Dev., 10(4), 1487–1520, doi:10.5194/gmd-10-1487-2017, 2017.
Williamson, A. G., Arnold, N. S., Banwell, A. F. and Willis, I. C.: A Fully Automated Supraglacial lake area and volume Tracking ("FAST") algorithm: Development and application using MODIS imagery of West Greenland, Remote Sens. Environ., 196, 113–133, doi:10.1016/j.rse.2017.04.032, 2017.
Williamson, A. G., Willis, I. C., Arnold, N. S. and Banwell, A. F.: Controls on rapid supraglacial lake drainage in West Greenland: an Exploratory Data Analysis approach, J. Glaciol., 1–19, doi:10.1017/jog.2018.8, 2018a.
Williamson, A. G., Banwell, A. F., Willis, I. C. and Arnold, N. S.: Dual-satellite (Sentinel-2 and Landsat 8) remote sensing of supraglacial lakes in Greenland, Cryosph. Discuss., 1–27, doi:10.5194/tc-2018-56, 2018b.
Winther, J.-G. G., Elvehøy, H., Bøggild, C. E., Sand, K. and Liston, G.: Melting, runoff and the formation of frozen lakes in a mixed snow and blue-ice field in Dronning Maud Land, Antarctica, J. Glaciol., 42(141), 271–278, doi:10.3189/s0022143000004135, 1996.
Wuite, J., Rott, H., Hetzenecker, M., Floricioiu, D., De Rydt, J., Gudmundsson, G. H., Nagler, T. and Kern, M.: Evolution of surface velocities and ice discharge of Larsen B outlet glaciers from 1995 to 2013, Cryosphere, 9(3), 957–969, doi:10.5194/tc-9-957-2015, 2015.
Yang, K. and Smith, L. C.: Supraglacial streams on the Greenland Ice Sheet delineated from combined spectral – shape information in high-resolution satellite imagery, IEEE Geosci. Remote Sens. Lett., 10(4), 801–805, doi:10.1109/LGRS.2012.2224316, 2013.

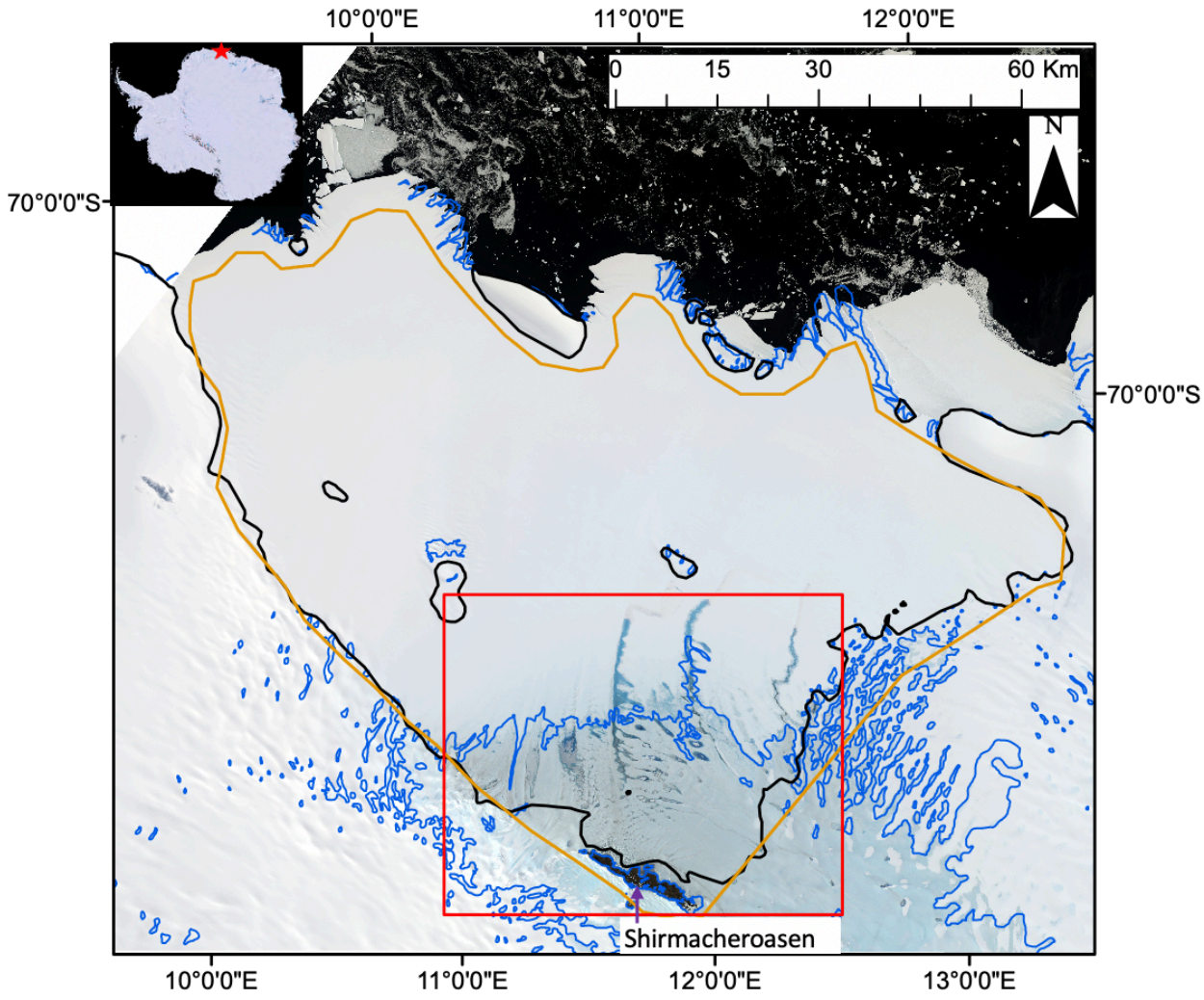

Figure 1: A map of the study area. The base image is a mosaicked RGB Sentinel-2 image of the Nivlisen Ice Shelf acquired on 26th January 2017. The solid black line marks the grounding line, according to the NASA Making Earth System Data Records for Use in Research Environments (MEaSUREs) Antarctic boundaries dataset (Mouginot et al., 2017). *The solid blue line represents the blue ice areas in the region according to* Hui et al. (2014). *The solid orange line shows the study area extent used for this study, and the solid red line marks the area shown in all subsequent figures. The red star on the inset shows the location of the Nivlisen Ice Shelf in the context of an image of Antarctica, which is a mosaic product based on sources from USGS, NASA, National Science Foundation, and the British Antarctic Survey (https://visibleearth.nasa.gov/view.php?id=78 592).*

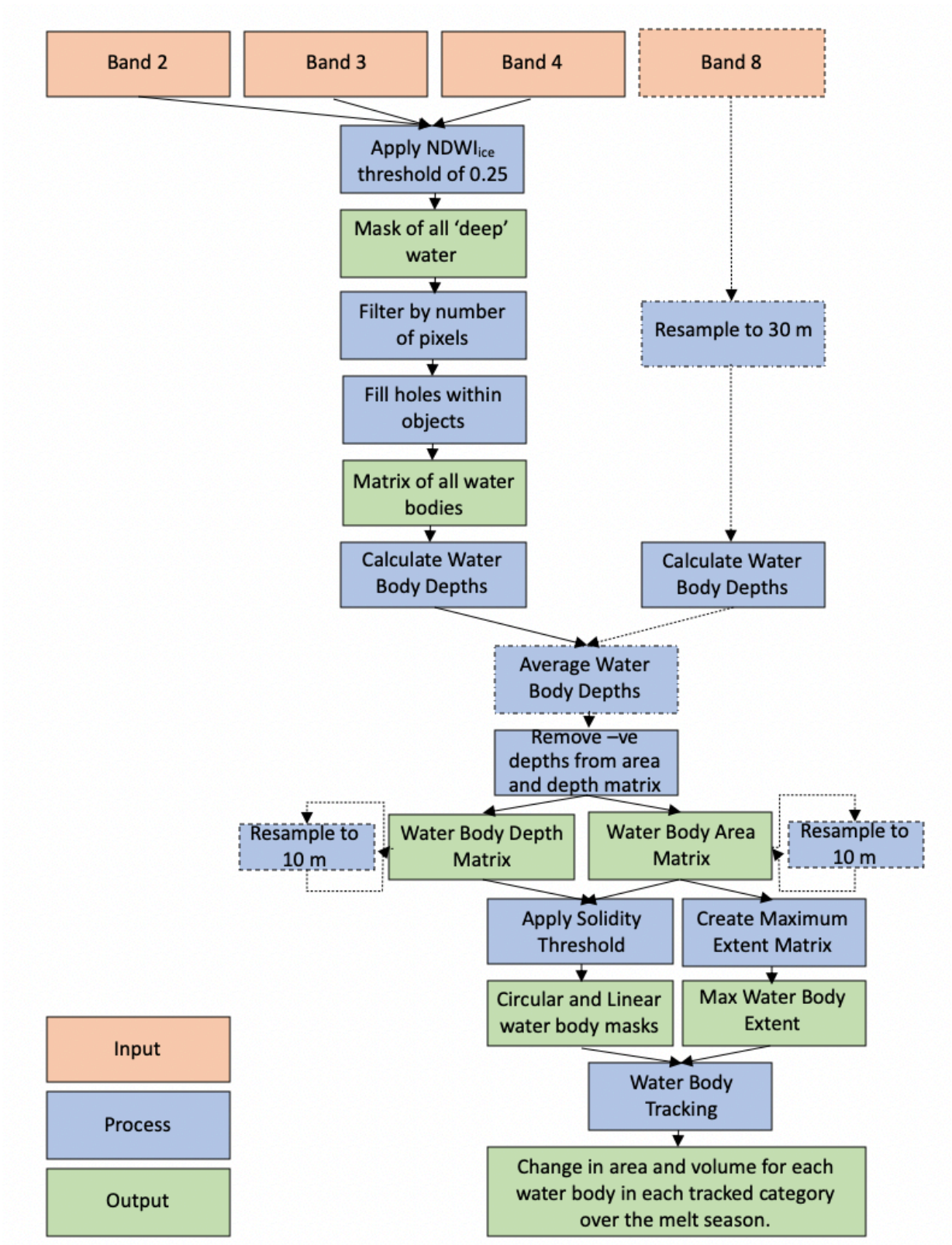

Figure 2: Workflow detailing the methods applied to both the Landsat 8 and Sentinel-2 images through the FASTISh algorithm in MATLAB. Dashed lines indicate steps that were applied to Landsat 8 images only, whereas solid lines indicate steps that were applied to both sets of image types. Modified from Williamson et al. (2018b).

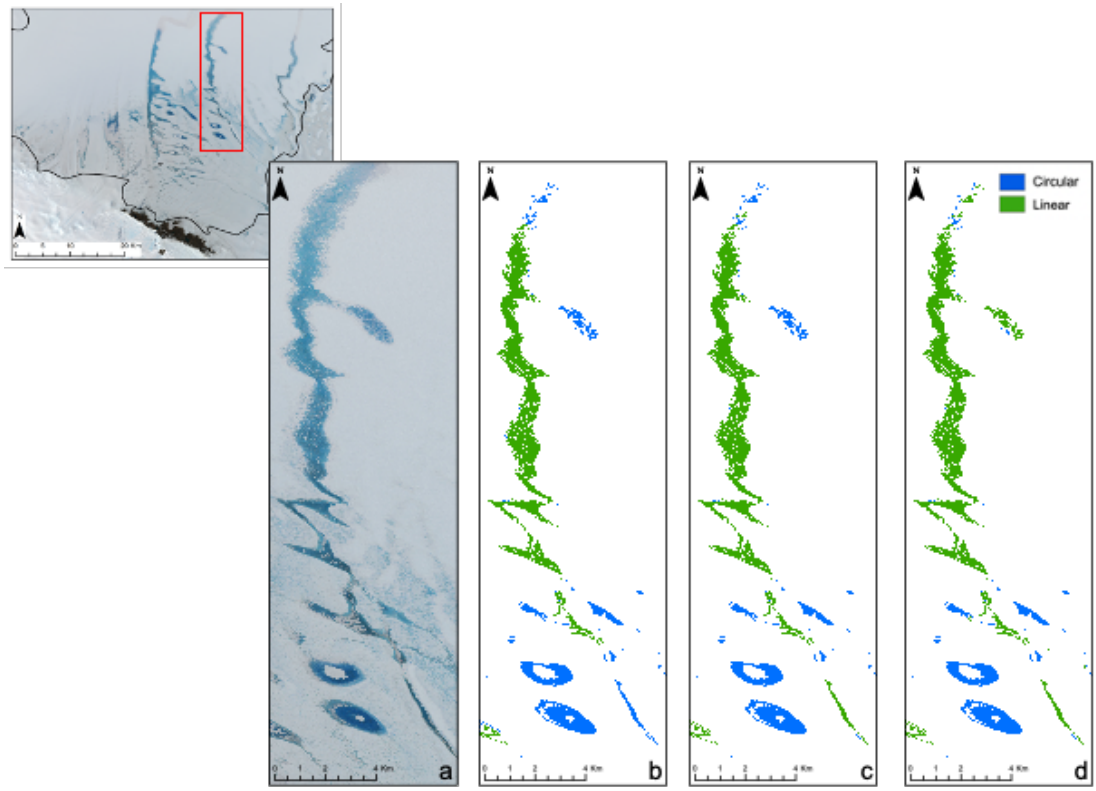

Figure 3: Solidity thresholds applied to water bodies identified on the Nivlisen Ice Shelf. The subset Sentinel-2 image is from the 26th January 2017, and the red box indicates the area shown in panels a-d. a) shows this area as an RGB, b) shows the water bodies identified and separated into linear or circular water bodies using a threshold of 0.42, c) a threshold of 0.45, and d) a threshold of 0.49.

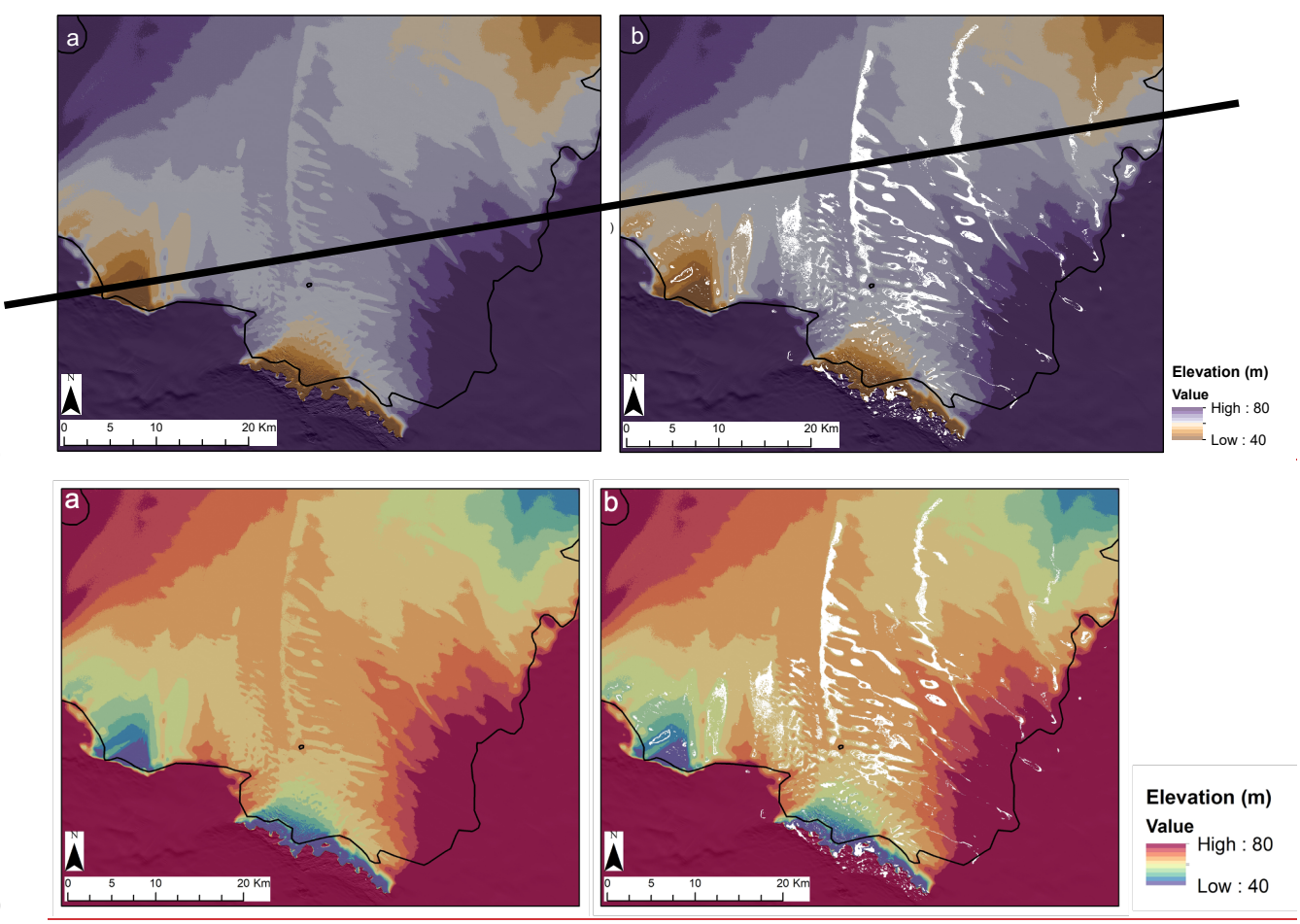

Figure 4: REMA DEM data for the Nivlisen Ice Shelf. a) the DEM; and b) overlain with the maximum melt extent matrix for the 2016-2017 melt season in white. DEM data sourced from the REMA dataset (Howat et al., 2019).

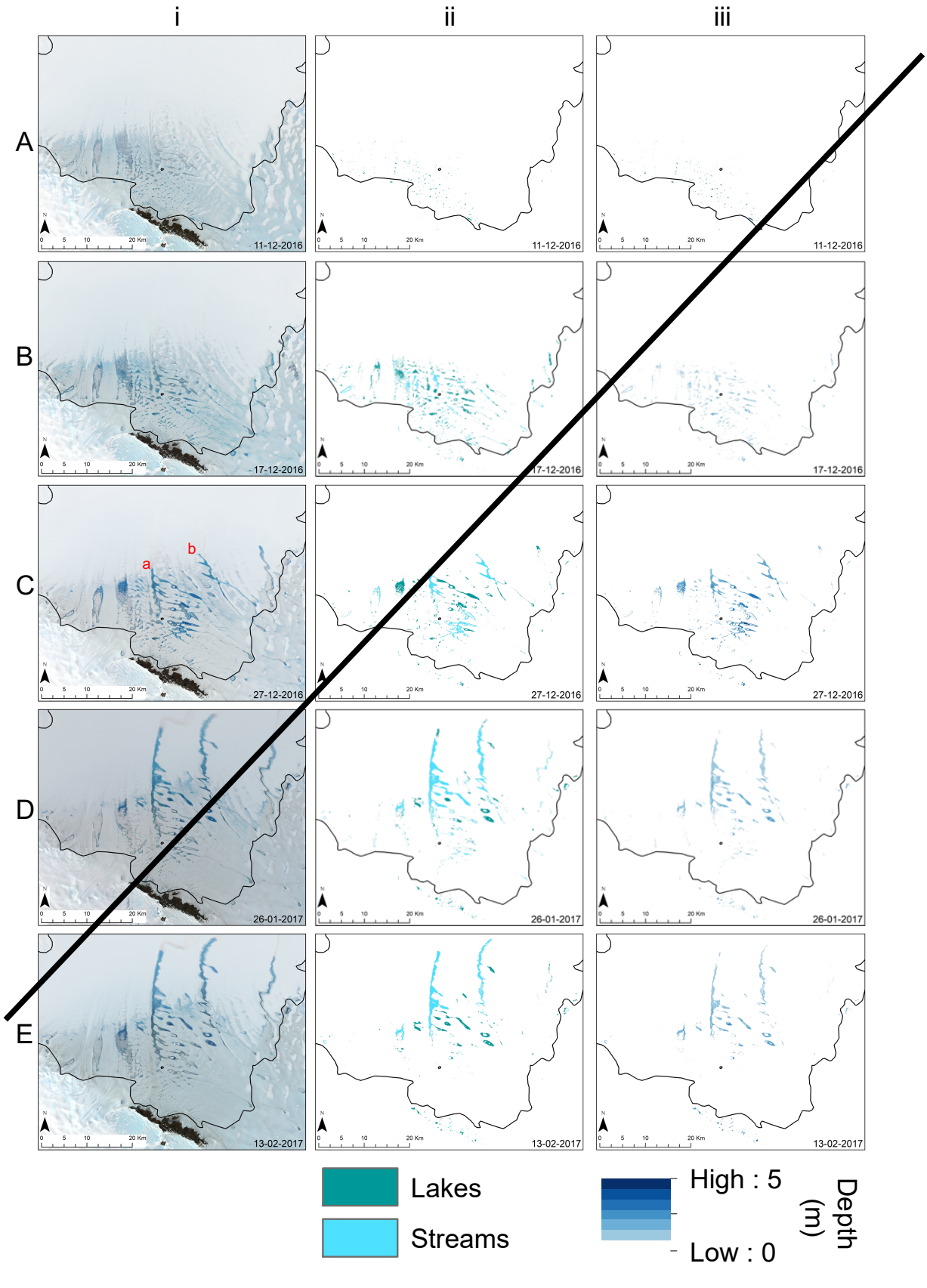
i
ii
iii
A
B
C
D
E
a
b
11-12-2016
17-12-2016
27-12-2016
26-01-2017
13-02-2017
Lakes
Streams
High : 5
Low : 0
Depth (m)

1037

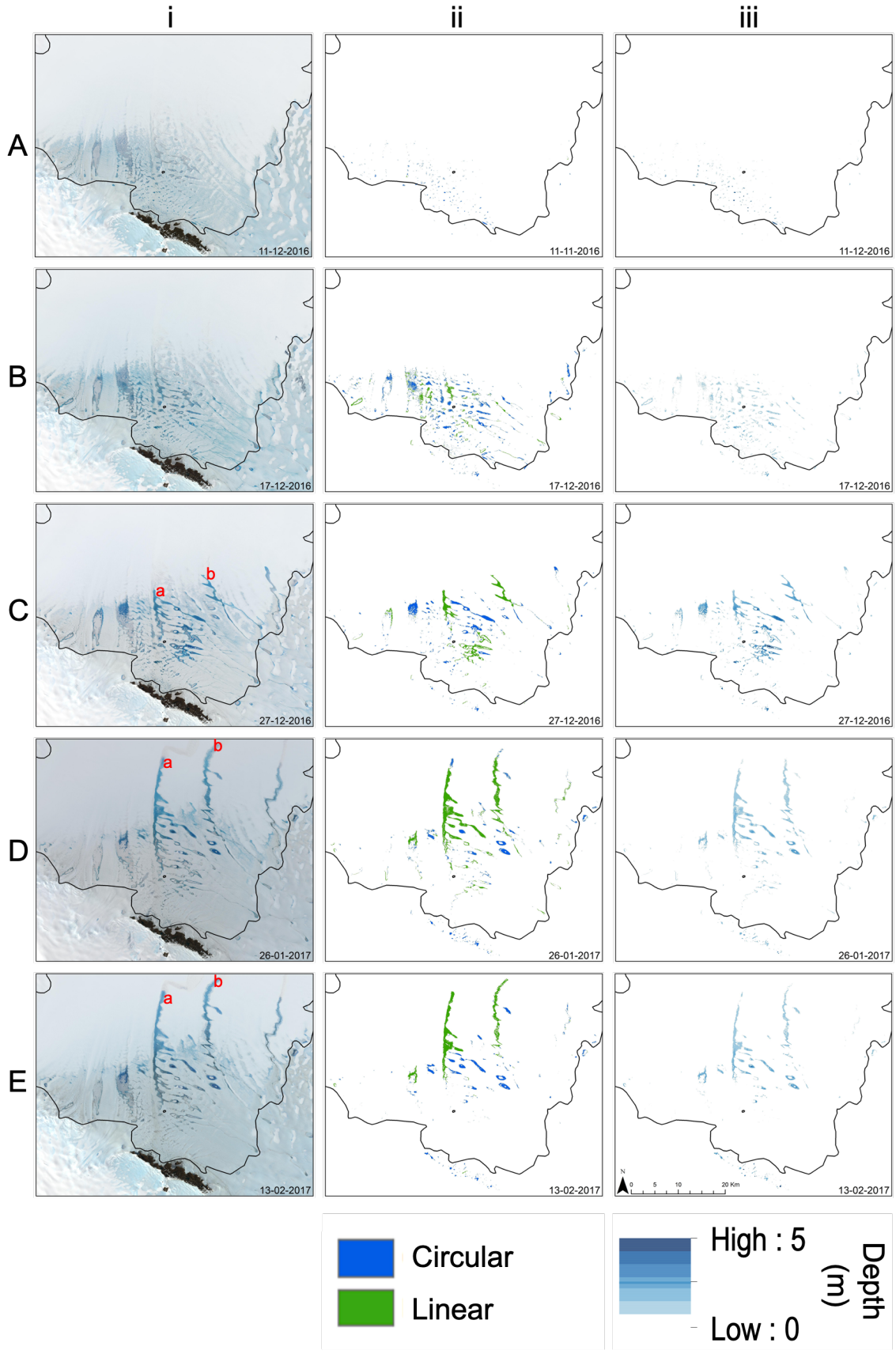

Figure 5: Five of the eleven dates studied in the 2016-2017 melt season (represented by labels A-E), and their corresponding (i) RGB images, (ii) lake and stream area masks, (iii) depth masks. See Fig. S2 for all RGB images, Fig. S3 for all lake and stream area masks and Fig. S4 for all depth masks produced in this study.

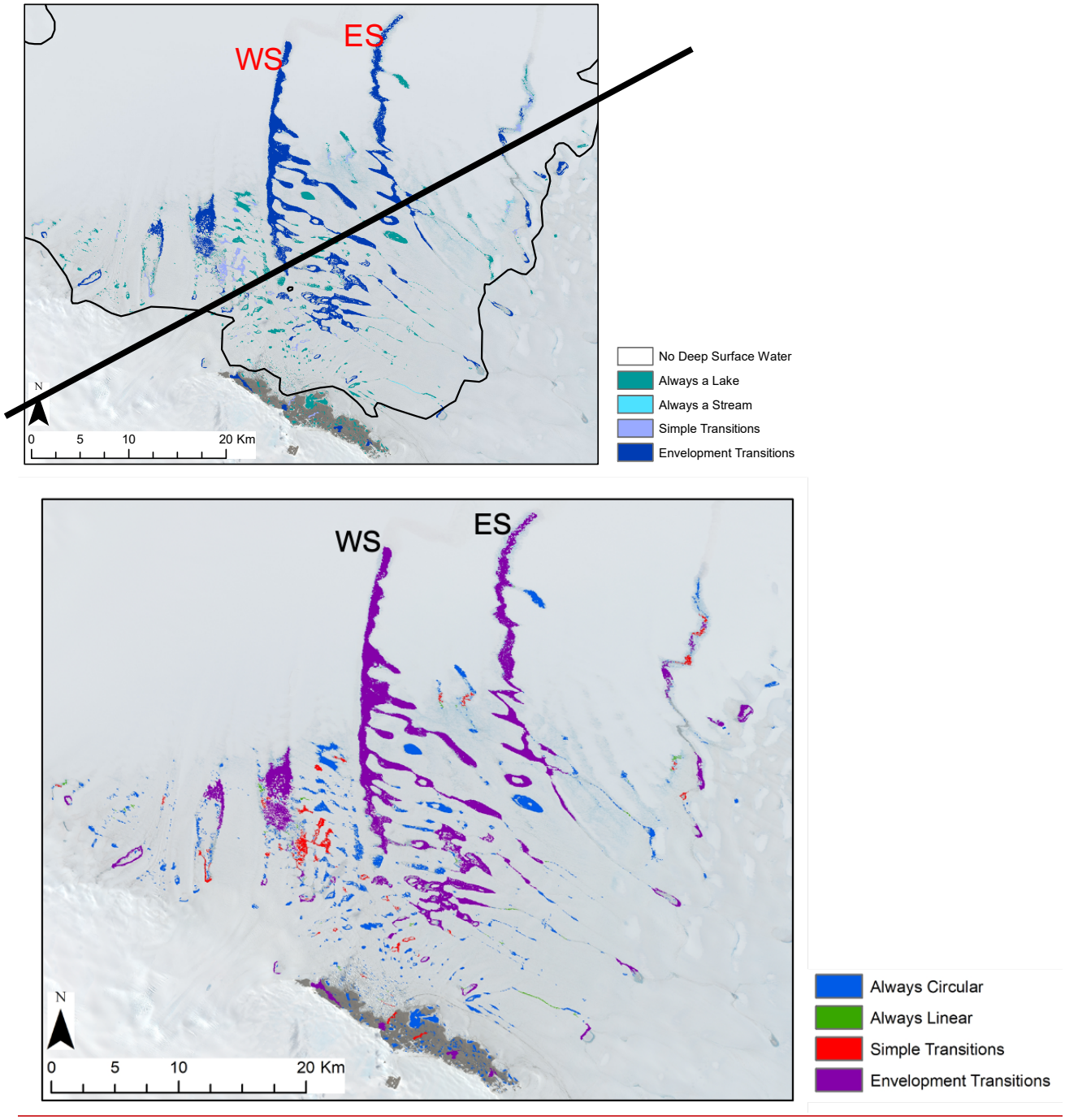

Figure 6: Maximum extent of all identified water bodies on the Nivlisen Ice Shelf for the 2016-2017 melt season, colour coded by water body type. 'WS' donates 'Western System', and 'ES' is Eastern System. Base image aquired by Sentinel-2 on 26th January 2017.

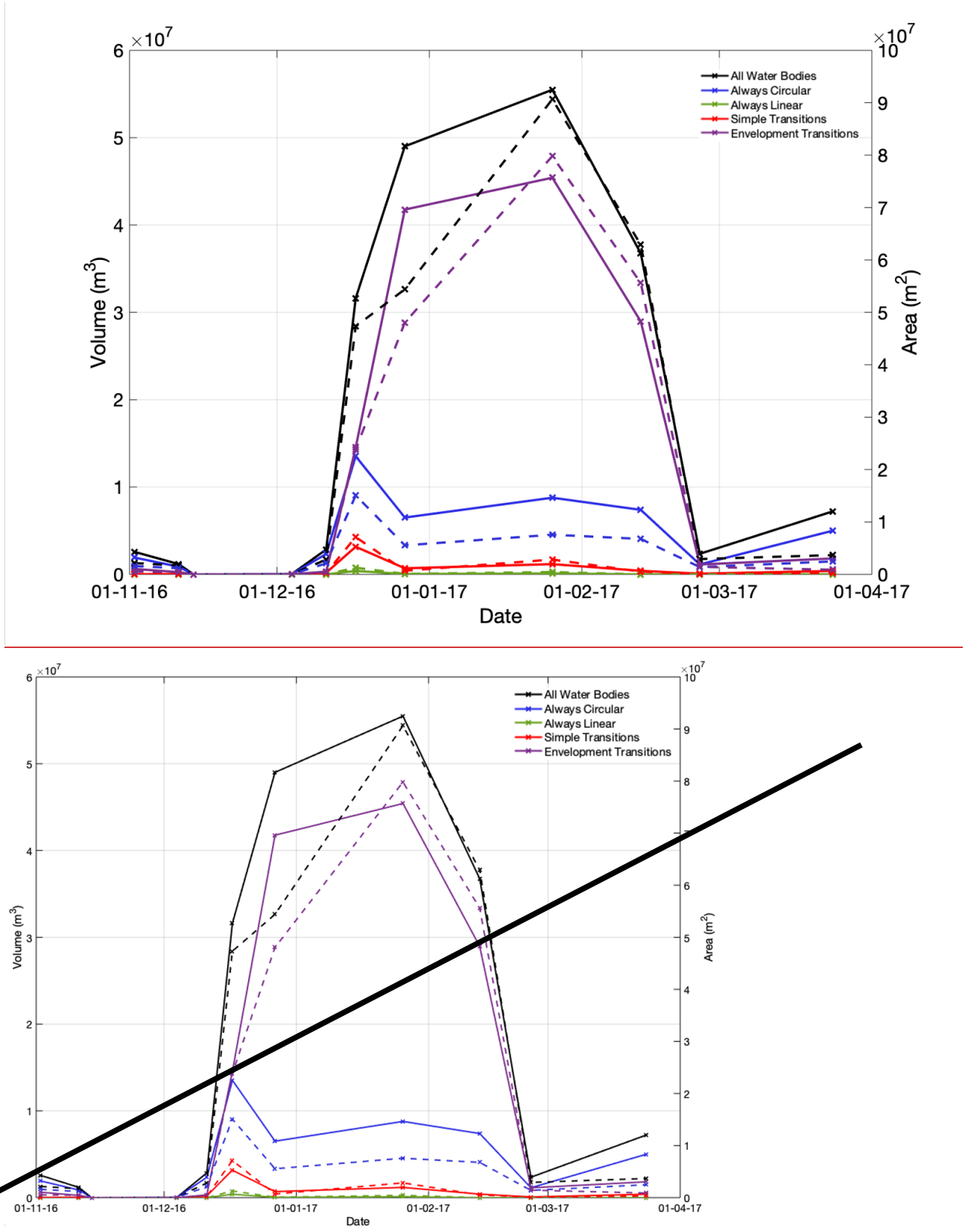

Figure 7: Time series of the total area and volume held in each water body category over the 2016-2017 melt season on the Nivlisen Ice Shelf. Volumes are indicated by the solid lines, and areas by the dashed lines.

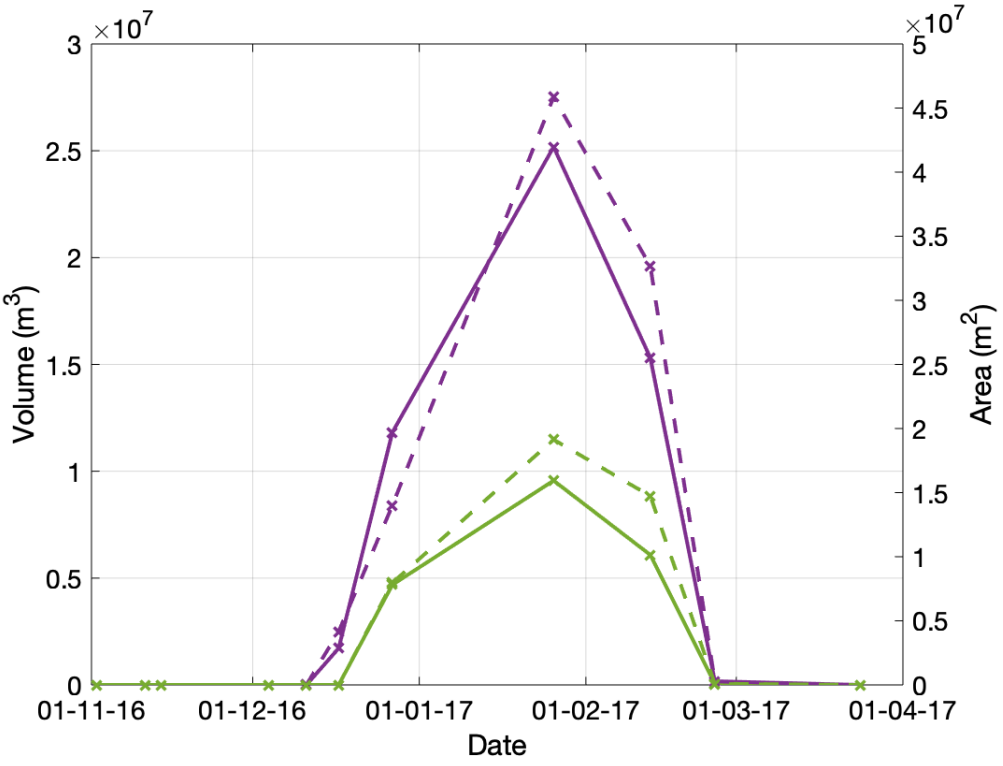

Figure 8: Time series showing the area (dashed line) and volume (solid line) of the WS (purple) and ES (green).

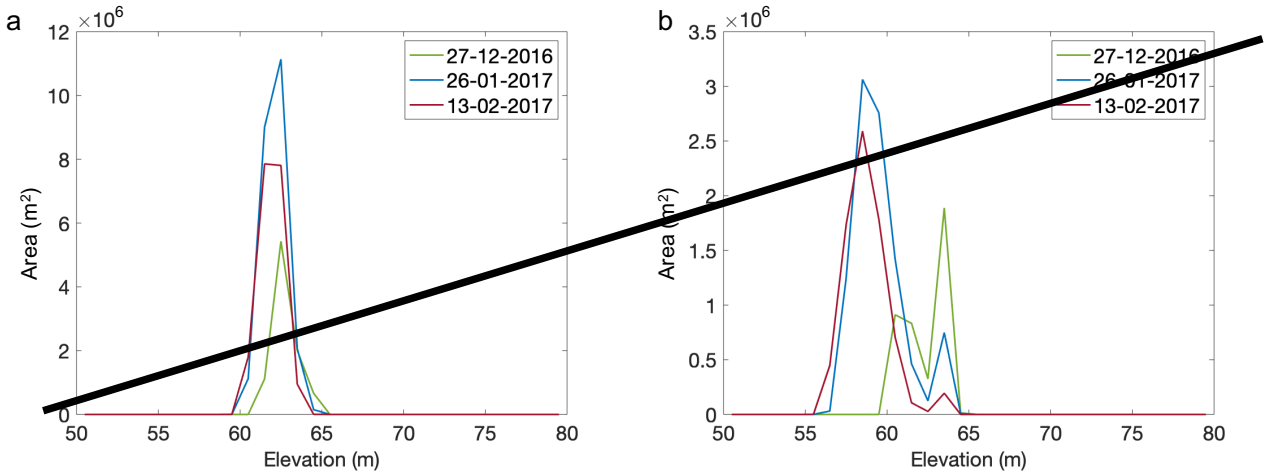

~~Figure 7: Elevation Distribution Plots for (a) the Western System (WS) and (b) the Eastern System (ES) on the Nivlisen Ice Shelf for three dates in the melt season. Data points are plotted at the mid-point of their elevation bins along the X axis.~~

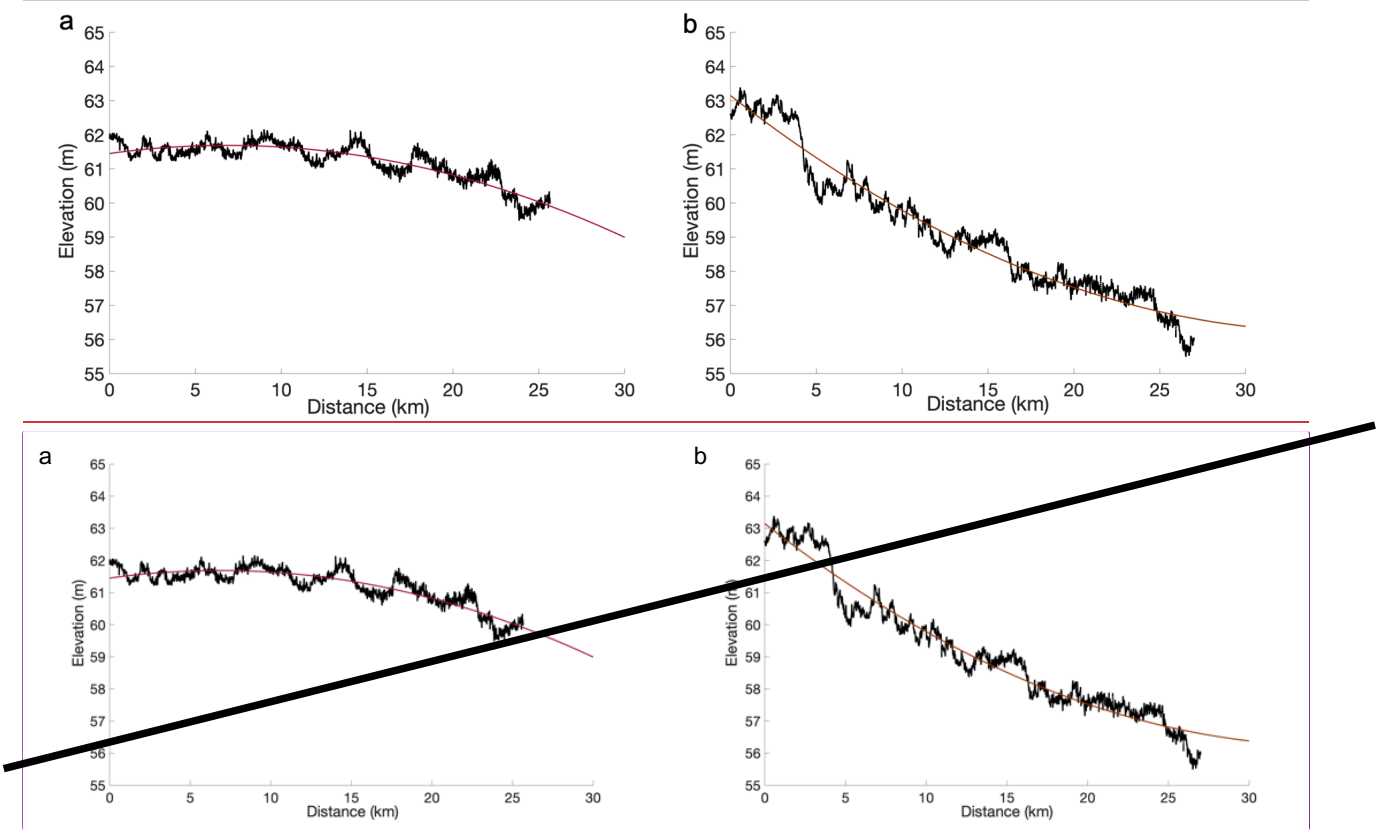

[IW1]

Figure 9: Elevation profiles for (a) the WS and (b) the ES. Quadratic trendlines are shown in red. Data are extracted from REMA (Howat et al., 2019) *and the path of data extraction was guided using the maximum depth matrix of both the WS and ES over the full 2016-2017 melt season (see Fig. S5).*

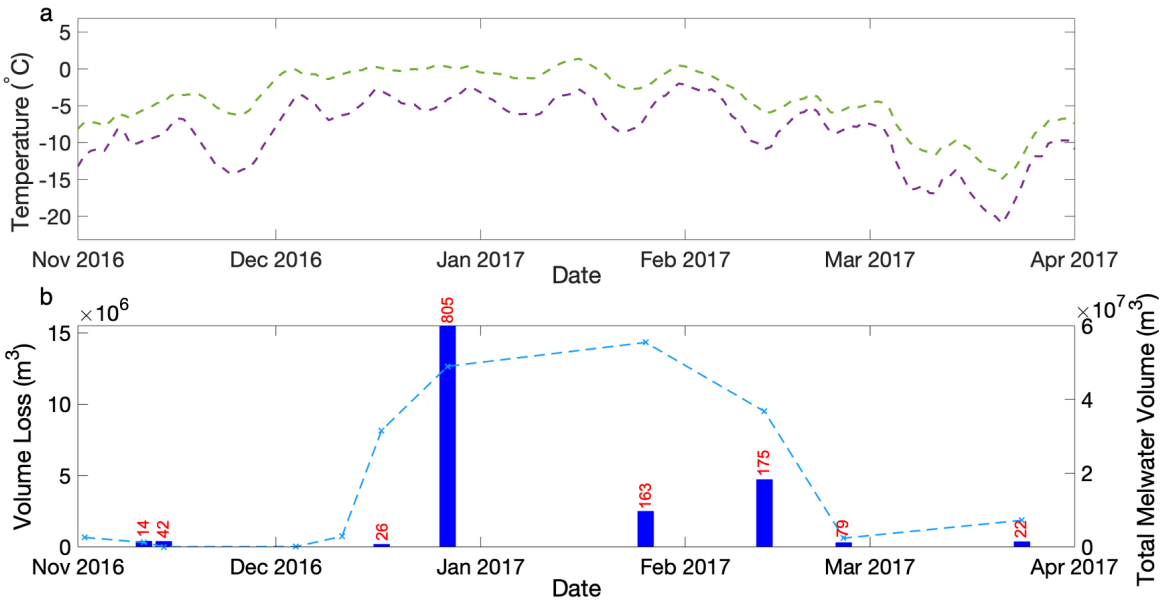

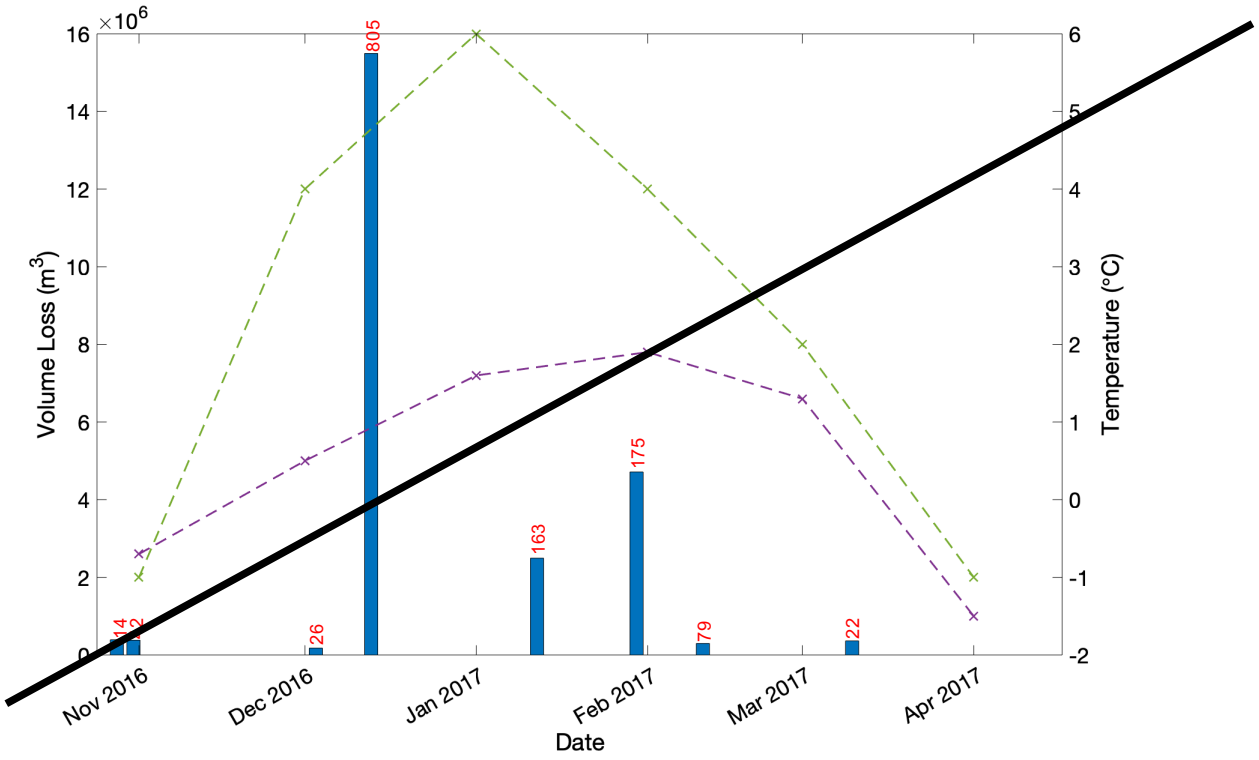

Figure 10: Meteorological context of circular lake loss events: a) The seven day moving average of mean daily (purple line) and daily maximum (green line) near-surface air temperature from the MetUM simulation for the period from November 2016 to April 2017 at the model point immediately to the south of Schirmacheroasen.b) The total volume lost in 'loss events' from water bodies in the 'always circular' category (blue bars) and the total combined water volume (blue line). A loss event is defined as a > 80 % loss in water body volume through either lake drainage or freeze-through. The total number of loss events for each date is indicated above each bar.

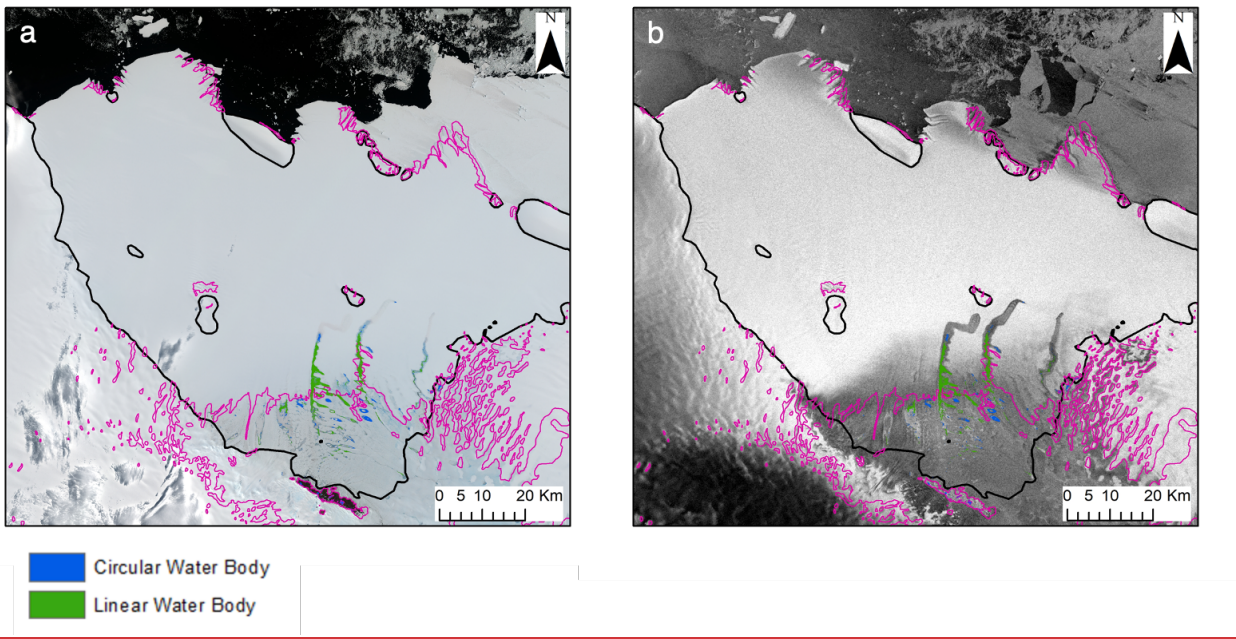

Figure 11: Comparison of optical imagery and radar imagery on 26th January 2017; a) is a mosaicked Sentinel-2 image, b) is a Sentinel-1 SAR image. Both a) and b) are overlain with the

blue ice extent (pink) and the mapped area of all linear and circular surface water bodies, based on the FASTISh analysis of (a).

Table 1: Total area, total volume, and mean depth of all meltwater bodies on the Nivlisen Ice Shelf on various dates in the 2016-2017 melt season.

Date	**Total Area (m^2)**	**Total Volume (m^3)**	**Mean Depth (m)**	**Max Depth (m)**
2nd November 2016	2.2×10^6	2.6×10^6	1.2	2.9
11th November 2016	1.7×10^6	1.2×10^6	0.7	2.6
14th November 2016	0.0	0.0	0.0	0.0
04th December 2016	4.4×10^4	4.0×10^4	0.9	3.1
11th December 2016	2.8×10^6	2.8×10^6	1.0	3.4
17th December 2016	4.7×10^7	3.2×10^7	0.7	3.1
27th December 2016	5.4×10^7	4.9×10^7	0.9	4.7
26th January 2017	9.1×10^7	5.5×10^7	0.6	3.3
13th February 2017	6.3×10^7	3.7×10^7	0.6	4.3
25th February 2017	2.9×10^6	2.4×10^6	0.8	3.0
24th March 2017	3.7×10^6	7.2×10^6	2.0	5.0

Table 2: Maximum Area and Volume for each water body category on the Nivlisen Ice Shelf on various dates in the 2016-2017 melt season.

	Maximum Area (m^2)	Maximum Volume (m^3)	Date of Maximum Volume	Date of Maximum Area
All Water Bodies	9.1×10^7	5.5×10^7	26th January 2017	26th January 2017
Always Lakes	1.5×10^7	1.4×10^7	17th December 2016	17th December 2016
Always Streams	1.3×10^6	3.9×10^5	17th December 2016	17th December 2016
Simple Transitions	3.2×10^6	3.2×10^6	17th December 2016	17th December 2016
Envelopment Transitions	8.0×10^7	4.5×10^7	26th January 2017	26th January 2017